Genome Analysis of Structure–Function Relationships in Respiratory Complex I, an Ancient Bioenergetic Enzyme

Mauro Degli Esposti[1,2,*]

[1]Italian Institute of Technology, Genova, Italy

[2]Center for Genomic Sciences, UNAM, Cuernavaca, Mexico

*Corresponding author: E-mail: Mauro.DegliEsposti@iit.it.

Accepted: November 24, 2015

Abstract

Respiratory complex I (NADH:ubiquinone oxidoreductase) is a ubiquitous bioenergetic enzyme formed by over 40 subunits in eukaryotes and a minimum of 11 subunits in bacteria. Recently, crystal structures have greatly advanced our knowledge of complex I but have not clarified the details of its reaction with ubiquinone (Q). This reaction is essential for bioenergy production and takes place in a large cavity embedded within a conserved module that is homologous to the catalytic core of Ni–Fe hydrogenases. However, how a hydrogenase core has evolved into the protonmotive Q reductase module of complex I has remained unclear. This work has exploited the abundant genomic information that is currently available to deduce structure–function relationships in complex I that indicate the evolutionary steps of Q reactivity and its adaptation to natural Q substrates. The results provide answers to fundamental questions regarding various aspects of complex I reaction with Q and help re-defining the old concept that this reaction may involve two Q or inhibitor sites. The re-definition leads to a simplified classification of the plethora of complex I inhibitors while throwing a new light on the evolution of the enzyme function.

Key words: bacterial evolution, mitochondria, respiratory complex I, NADH-ubiquinone oxidoreductase, ubiquinone, respiratory inhibitors.

Introduction

Respiratory complex I is the common name of a large enzyme complex that transports electrons from NADH to ubiquinone (Q), NADH:ubiquinone oxidoreductase (Nuo), EC. 1.6.5.3. Contrary to other NADH dehydrogenases, complex I couples the transport of electrons to the generation of membrane potential by pumping two protons per electron across the membrane in which the enzyme complex resides (either the bacterial plasma membrane or the inner membrane of mitochondria; Brandt 2006; Sazanov 2015). Complex I can also catalyze NAD+ reduction from reduced Q, QH_2 (Gutman et al 1970; Dupuis et al 1998; Grivennikova et al 2003), consuming membrane potential to drive the energetically unfavorable reaction (the redox midpoint potential of NADH being −0.34 V, whereas that of Q/QH_2 normally around +0.1 V; Brandt 2006; Sazanov 2015).

The recent three-dimensional (3D) structural information produced by Sazanov and co-workers on bacterial complex I (Sazanov and Hinchcliffe 2006; Baradaran et al. 2013; Sazanov 2015) and by others on mitochondrial complex I (Vinothkumar et al. 2014; Zickermann et al. 2015) has confirmed previously noted homologies with bacterial enzymes such as hydrogenases (Fearnley and Walker 1992; Oh and Bowien 1998; Baumer et al. 2000; Friedrich and Scheide2000), reinforcing the concept that complex I has a modular design (Moparthi and Hägerhäll 2011; Sazanov 2015). Three physically distinct modules are named after the enzyme substrates (N for NADH and Q for quinone) and the proton pumping function in the membrane (P for proton) (Moparthi and Hägerhäll 2011; Marreiros et al. 2013; Sazanov 2015). The evolution of complex I is thought to have followed a progressive assembly of these modules derived from diverse enzyme systems, with the combination of the Q and P module resembling the structure of membrane-bound Ni–Fe hydrogenases (Friedrich and Scheide 2000; Hedderich 2004; Efremov and Sazanov 2012; Marreiros et al. 2013). The subsequent acquisition of the N module would have produced the minimal enzyme structure conforming to mitochondrial complex I, which in bacteria is coded by *nuo* operons of 13 or 14 subunits (Dupuis et al. 1998; Friedrich and Scheide 2000; Moparthi and Hägerhäll 2011; Sazanov 2015; Spero et al. 2015). In eukaryotes, many accessory

subunits have been added to facilitate the assembly and regulation of mitochondrial complex I (Fearnley and Walker 1992; Brandt 2006; Yip et al. 2011; Vinothkumar et al. 2014; Zickermann et al. 2015). However, the redox and bioenergetic function is essentially the same in the bacterial and mitochondrial enzyme complexes (Yagi et al. 1998).

Even if bacterial Nuo complexes reflect the core structure of mitochondrial complex I (Friedrich and Scheide 2000; Brandt 2006; Sazanov 2015), the 3D information that is currently available shows a remarkable difference in the binding pocket for Q and its antagonist inhibitors (Sazanov 2015). The crystal structure of the complex from *Thermus*, a thermophilic bacterium of the ancient *Deinococcus/Thermus* phylum (Segata et al. 2013), has revealed an unusually large reaction chamber with a narrow entrance within the Q module lying at the membrane periphery, in which exogenous Q (decyl-ubiquinone, DBQ) is hydrogen-bonded to conserved H38 and Y87 of the NuoD subunit (Baradaran et al. 2013). These structural features are illustrated in fig. 1*A*, which highlights key residues of the Q reaction chamber that will be analyzed here. The potent Q antagonist inhibitor piericidin A (Takahashi et al. 1965) is bound in the same way within the Q reaction chamber of *Thermus* (Baradaran et al. 2013; Sazanov 2015) (fig. 1*A*, right panel). However, the structure of mitochondrial complex I from the fungus *Yarrowia* shows a narrower Q binding pocket, in which the Q antagonist inhibitor DQA (2-decyl-4-quinazolinyl amine, previously known as SAN 547; Hollingworth et al. 1994; Degli Esposti 1998; Okun et al. 1999) is hydrogen-bonded to a histidine residue of the 49-kDa subunit that corresponds to H38 in the NuoD of *Thermus*, but is far away from the tyrosine residue equivalent to *Thermus* Y87, as sketched in fig. 1*A*, right panel (Zickermann et al. 2015). The possibility that this binding difference is owing to the so-called deactive state in which the *Yarrowia* complex is isolated (Zickermann et al. 2015 cf. Galkin et al. 2008) apparently contradicts biochemical results showing very strong resistance toward DQA inhibition in *Yarrowia* and *E. coli* complex I after mutation of the residues equivalent to *Thermus* Y87 (Kashani-Poor et al. 2001; Tocilescu et al. 2010b; Sinha et al. 2015).

The simplest explanation for the different binding of Q and its antagonists in the structure of bacterial (*Thermus*) and mitochondrial (*Yarrowia*) complex I (cf. fig. 1*A*) would be that the Q module can simultaneously bind two molecules of Q or antagonists such as DQA and related quinazoline inhibitors (Degli Esposti et al. 1999; Murai et al. 2009; Verkhovsky et al. 2012). This possibility would be consistent with a wealth of biochemical data and with the structural evidence that the Q reaction chamber in *Thermus* complex I is wide enough to accommodate two short-chain Q homologs such as Q-1 or Q-2 (Baradaran et al. 2013). These quinones retain functional activity after mutation of Y87 (Tocilescu et al. 2010b; Sinha et al. 2015) and consequently can bind to another side of the Q chamber. The same chamber could equally accommodate two molecules of the Q antagonist piericidin, which has a structure very similar to Q-2 (Takahashi et al. 1965; fig. 6)—even if the conditions of crystallization may allow saturation only of the tighter of the two sites in *Thermus* (Baradaran et al. 2013). For a long time, piericidin has been known to bind to two sites in mammalian and fungal complex I (Gutman et al. 1970; Coles et al. 1974; Singer and Ramsay 1994) and to potently inhibit also bacterial complex I (Friedrich et al. 1994; Dupuis et al. 1998). This evidence suggested that mitochondrial complex I may have two Q reaction sites (Friedrich et al 1994; Degli Esposti et al. 1996; Magnitsky et al. 2002; Ohshima et al. 1998; Verkhovsky et al. 2012), a concept that has been subsequently weakened by mutagenesis (Brandt 2006; Tocilescu et al. 2010b) and structural (Baradaran et al. 2013) studies.

Mutually exclusive binding of complex I inhibitors can now be rationalized on the basis of the unique features of the Q reaction chamber. The structure of both bacterial (Baradaran et al. 2013) and mitochondrial (Zickermann et al. 2015) complex I shows a narrow entry channel for Q coming from the membrane. Hence, the long isoprenoid tail of natural Q substrates locks them within the wormhole-like entry site from the membrane, whereas their hydrophilic head (and initial prenyl groups) acquires freedom of movement upon penetrating the wide reaction chamber formed by the subunits of the Q module. Movements of Q within the chamber are likely to contribute to the conformational changes that couple redox reactions to proton pumping (Sazanov 2015; Sharma et al. 2015). Most antagonist inhibitors mimic the hydrophilic head of Q substrates but match only partially their hydrophobic tail, as they usually are not much longer than Q-2 (Ohshima et al. 1998; Murai et al. 2009, cf. fig. 6). Notably, Q-2 acts a product-like inhibitor in mammalian complex I (Lenaz et al. 1968; Degli Esposti 1998; Ohshima et al. 1998). Hence, multiple Q antagonist molecules may penetrate one at a time the wormhole-like entry in complex I and then accumulate inside the Q-reacting chamber.

The considerations just discussed have stimulated the present work that has followed genomic and evolutionary approaches to deduce crucial structure–function relationships of complex I interaction with quinones. The analysis has been integrated with functional studies to answer the fundamental question of how Q reactivity emerged along evolution. Because crystal structures of complex I show a single Q binding pocket that is enclosed within the NuoD protein at its interface with the NuoB and NuoH subunits (fig. 1*A*, cf. Sazanov 2015), it can be assumed that Q reactivity evolved primarily within the NuoD subunit. Key amino acids facing its internal cavity (fig. 1*A*, right panel) that originally contained the Ni–Fe cofactor of hydrogenases would then change in concert with others lying in the regions interconnected with the NuoB and NuoH subunits, together forming the Q reaction chamber (Baradaran et al. 2013). Detailed sequence analysis of these subunits should then reveal the key amino acid

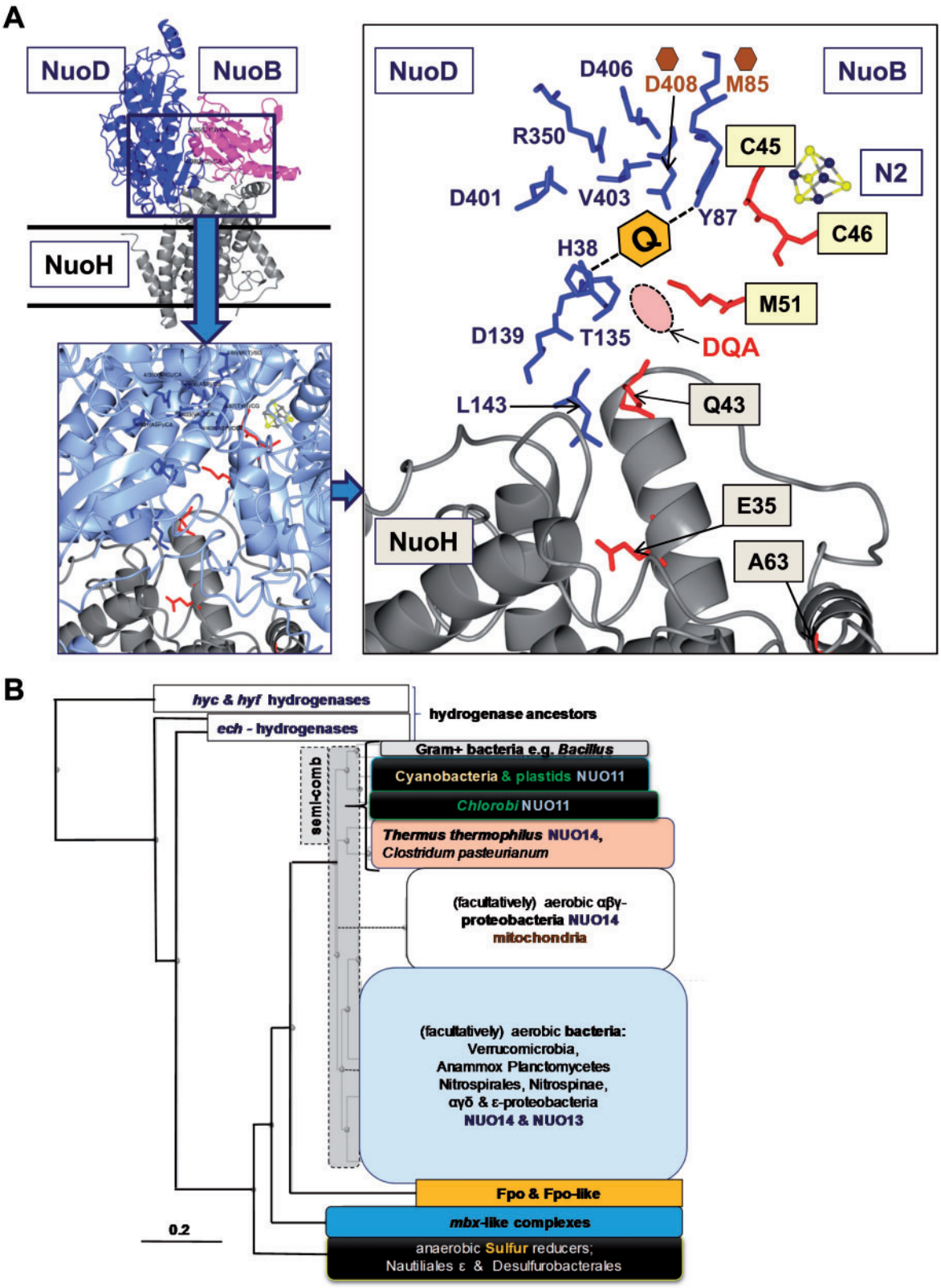

FIG. 1.—Structure and evolution of complex I. (*A*) 3D image of Q-interacting subunits and residues in complex I. The ribbon model of the subunits forming the Q reaction chamber in *Thermus* complex I (top panel on the left, cf. Baradaran et al. 2013) is zoomed in and slightly tilted to the left in the bottom panel. It is then enlarged in the right panel, in which the overall structures of NuoD and NuoB were removed, while rendering in cylinder mode most residues

(continued)

signatures that are linked to the acquisition of Q reactivity from homologous proteins of Ni–Fe hydrogenases, which do not react with membrane quinones. Following this rationale, the investigation has been expanded to answer the questions:

1. Which of these signatures correspond to Q-binding residues in the 3D structure of bacterial and mitochondrial complex I?
2. Are natural substitutions of these residues related to different quinone types that are present in some archaea and bacteria?
3. Do organisms that produce complex I inhibitors show substitutions of (or near to) these residues that could account for natural resistance of their complex I toward the same Q antagonist inhibitors?

The results presented below provide answers to these questions while throwing a new light on the evolution of the structure and function of respiratory complex I.

Results and Discussion

A novel pattern for the evolution of bacterial complex I

Phylogenetic trees based on the highly conserved NuoD/49 kDa/Nad7 subunit of complex I (fig. 1*B*) produced novel information to interpret the possible evolution of Nuo complexes that is of relevance to the acquisition of Q reactivity. Previous models for the evolution of complex I proposed that membrane-bound hydrogenases such as *E. coli hyc* (Vignais and Billoud 2007) may either be the progenitors of complex I (Fearnley and Walker 1992; Hedderich 2004) or have a common ancestral origin with Nuo complexes (Moparthi and Hägerhäll 2011). Alternatively, subtypes of group 4 hydrogenases that lack canonical Ni-Fe ligands, such as *ehr* (energy converting hydrogenase-related complexes—Marreiros et al. 2013) and *hyq* (hydrogenases quinone reacting in alpha proteobacterial diazotrophs; Sprecher et al. 2012), have been proposed as intermediates in the evolution of complex I. By contrast, the present analysis suggests that the large subunit of group 4 hydrogenases of the *ech* subtype (energy converting hydrogenases, e.g., CO-induced Ni–Fe hydrogenase of *Rhodospirillum rubrum*; Coppi 2005; Drennan et al. 2007) may be the precursors of NuoD (figs. 1*B* and 2, cf. Kashani-Poor et al. 2001).

The most ancestral forms of *nuo* operons are found in organisms that thrive in oceanic hydrothermal vents: members of the Nautiliales order of epsilon proteobacteria (Campbell et al. 2009) and the deep-branching *Desulfurobacterium* and *Thermovibrio* of the *phylum* Aquificae, now grouped in the order of Desulfurobacteriales (Göker et al. 2011; Giovannelli et al. 2012). These strictly anaerobic organisms share the pathways of H_2-mediated sulfur reduction and reverse tricarboxylic acid cycle (Campbell and Cary 2004; Campbell et al. 2009), which is present also in facultatively anaerobic organisms such as *Thermotoga* and *Magnetococcus* (Schübbe et al. 2009) that possess a partial *nuo* operon matching the *mbx* complex originally found in *Pyrococcus*.

Pyrococcus mbx complex functions to support ferredoxin-reducing hydrogenases, re-oxidizing reduced ferredoxin to produce NADPH for biosynthetic purposes when elementary sulfur is available as final electron acceptor (Bridger et al. 2011). The gene sequence of such a complex incorporates the entire operon of a *pha/mrp* antiporter system (cf. fig. 2*A*) and uses the Fe–S clusters in the homolog of the NuoI subunit to directly reduce NADP+. In the *mbx*-like operon of *Thermotoga* and proteobacteria, instead, the NuoI subunit is substituted by a flavoprotein related to *gltD* (fig. 2*B*), the small subunit of NAD(P)-dependent glutamate synthase interacting with NAD(P)H (Suzuki et al. 2005). Hence, this subunit functions as the reduction site for the acceptor substrate NAD(P)+, while the *mbx*-like operon often terminates with rubrerythrin (fig. 2*B*), a redox protein probably involved in quenching radicals (Sztukowska et al. 2002). The NuoD homologs of *mbx* and *mbx*-like complexes show the vestigial presence of Cys residues at positions corresponding to cysteine ligands of the

Fig. 1.—Continued

that interact with Q or form its reaction chamber (Sazanov 2015). The residues belonging to the NuoD subunit are colored in blue or brown, whereas those of NuoB and NuoH are in red. The position of the quinone head of bound DBQ is indicated by the orange hexagon, with the dashed lines indicating the approximate position of the hydrogen bonds between the quinone carbonyls and Y87 and H38 (Baradaran et al. 2013). The dashed oval indicates instead the approximate position of the Q antagonist DQA bound to *Yarrowia* complex I (Zickermann et al. 2015). The brown hexagons on top of residues D401 and M85, also colored in brown, indicate the involvement of such residues in natural or induced resistance to the Q antagonist piericidin A (table 3), even if they were not listed among the Q-interacting amino acids in *Thermus* complex I (Baradaran et al. 2013). At the bottom of the right panel, A63 is shown; it frames the entrance into the reaction chamber from the wormhole through which Q penetrates the complex from the membrane (Baradaran et al. 2013). (*B*) Phylogenetically wide tree of the NuoD/Nad7/49 kDa subunit. The neighbor-joining (NJ) tree was initially obtained using the deltaBLAST program (Boratyn et al. 2012; Degli Esposti et al. 2015) using NuoD of *Nitrospira defluvii* (accession number: CBK40385) as the query and was extended to 5,000 sequences from bacteria and archaea possessing simplified Nuo operons. Note that after the early, well-separated branching groups of sulfur-reducing anaerobes (such as Nautiliales) and *mbx*-like complexes (which appear to be sister groups in trees of other Nuo subunits), as well as that of Fpo complexes, the proteins from other bacterial phyla are not well-resolved from each other, thus forming a semi-comb pattern of clades (Bapteste et al. 2008). Only the central group of alpha, beta, and gamma proteobacteria, corresponding to clade A and B in Spero et al. (2015) and encompassing also the eukaryotic homologs, is resolved as an independent branch. Nevertheless, the NuoD of *Chlorobi*, some gram-positive bacteria such as *Bacillus cereus* and *Clostridium pasteurianum*, as well as of plastidial NDH-1 group together in an early diverging branch containing Q-reacting NUO11 complexes. The tree is rooted on group 3 hydrogenases from *E. coli* (Vignais and Billoud 2007), while *ech* hydrogenases form the immediate precursor branch for complex I clades.

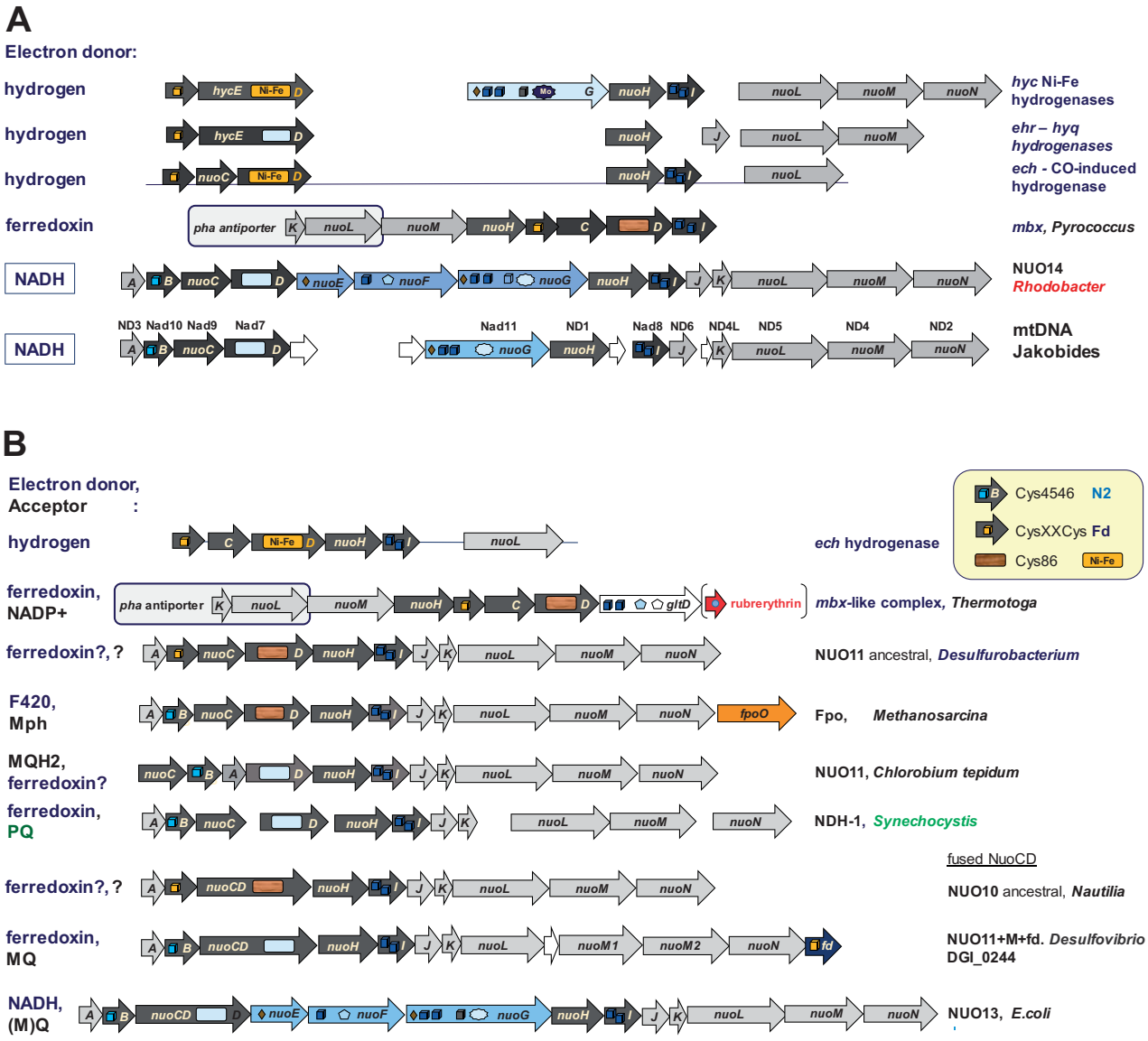

Fig. 2.—Gene clusters for Nuo complexes and their ancestors. (*A*) Graphical illustration of the gene clusters for membrane-bound hydrogenases and a typical complete *nuo* operon for complex I. The *nuo* operon of *Rhodobacter capsulatus* has been simplified by removing open reading frames that intermix with the canonical Nuo subunits (Dupuis et al. 1988). The *ech* type hydrogenase corresponds to the CO-induced enzyme of *R. rubrum* (Drennan et al. 2007), whereas the gene sequence at the bottom labeled "mtDNA Jakobides" represents the synthenic groups of complex I subunits in the mitochondrial genome of the jakobide *Andalucia* (Burger et al. 2013). Genes are color-coded as follows: light gray, P-module; dark gray, Q-module; light blue, N-module. The light blue rectangle inside NuoD subunits indicates the loss of ligands for the Ni–Fe cluster of hydrogenases. (*B*) Possible evolution of *nuo* gene sequences. The earliest recognizable sequence of NUO11 operons for complex I is seen in *Desulfurobacterium* (top part) or, when NuoD is fused with NuoC, in *Nautilia* (bottom part); these bacteria, therefore, have the most ancestral form of the complex, which is similar to that present in MQ-reacting NUO11 of *Chlorobium* and the PQ-reacting NDH-1 complex of Cyanobacteria such as *Synechocystis* (which is split in different synthenic groups and additionally has small subunits involved in ferredoxin binding that are not shown here; Ma and Ogawa 2015). The legend on the top right indicates the different symbols used for cluster N2 ligated to two consecutive cysteines in the NuoB subunit (light blue cube, cf. fig. 1*A*), the homologous high-potential Fe_4S_4 clusters of hydrogenases and ancestral Nuo operons (yellow cube) (table 2), and NuoD proteins retaining the first (Cys86 with *Thermus* numeration) and third ligand of the Ni–Fe cluster of hydrogenases (fig. 3*A* and table 1). Other symbols are as follows: pentagons, flavin cofactors; dark stars with Mo inside, Mo-binding domains; gray stars without Mo, lost Mo-binding domains; dark diamonds, F_2S_2 clusters; dark blue cubes, Fe_4S_4 clusters in subunits NuoF, NuoG, and NuoI; gray dashed cube, cluster N7 present in *Thermus* and other bacteria (Pohl et al. 2007; Sazanov 2015). The known or likely substrates are indicated on the left of each gene sequence. Additional variations in Nuo gene clusters are shown in supplementary fig. S2, Supplementary Material online.

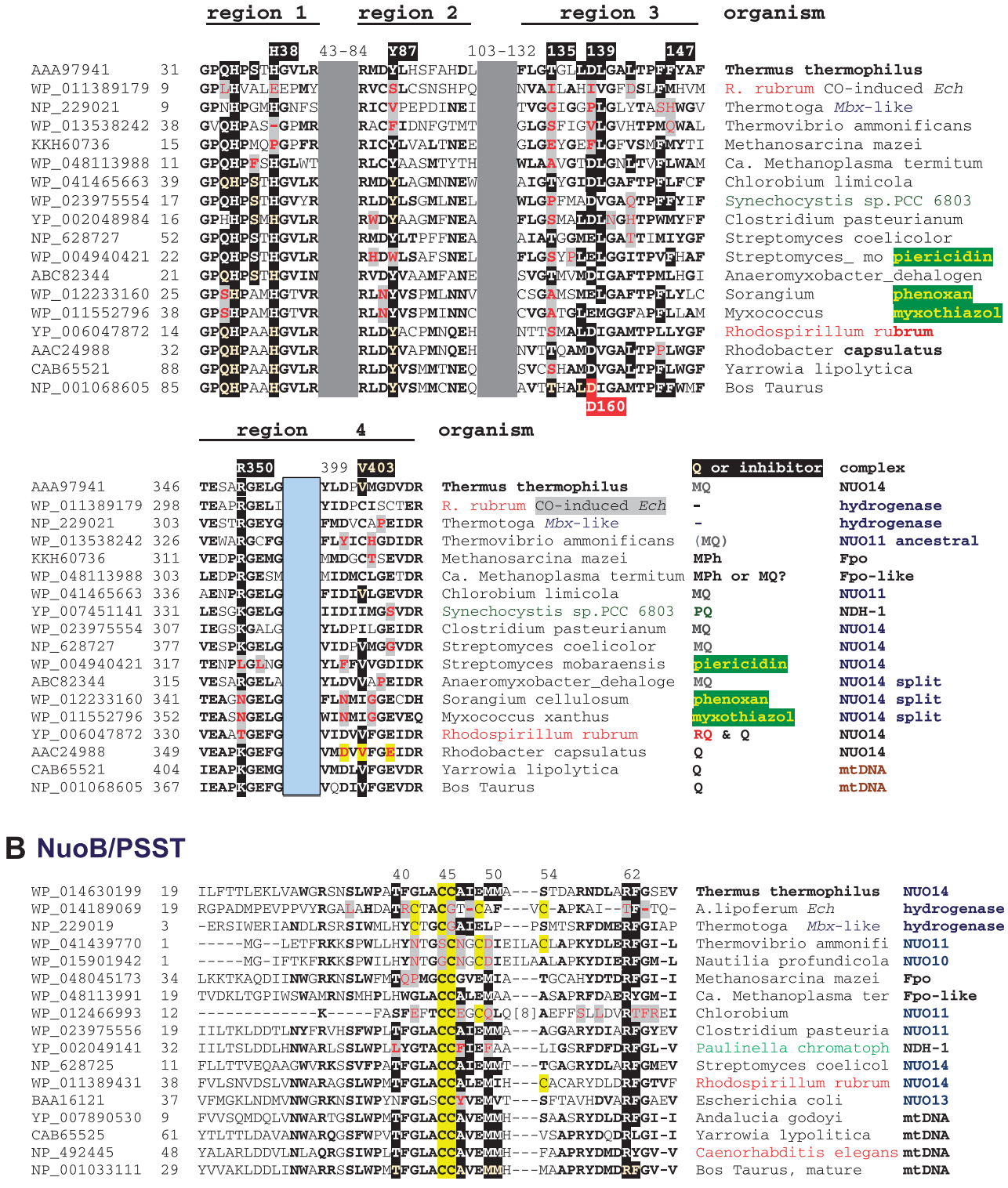

FIG. 3.—Alignment of NuoD/Nad7/49-kDa subunit sequences of complex I and acquisition of Q reactivity in complex I. Sequences with the accession number identified on the left were first aligned using the COBALT feature of the BLAST program and then manually refined (Degli Esposti et al. 2015). (*A*) Alignment blocks of the NuoD/49-kDa subunit showing the four conserved regions that contribute to the architecture of the large Q reaction chamber. The four conserved regions are indicated on top of the alignment and the type of complex is identified on the right. The quinone substrates or the Q antagonist

(continued)

Ni–Fe cluster of hydrogenases (fig. 3), a feature shared with archean Fpo (F420-phenazine oxidoreductase) complexes (Moparthi and Hägerhäll 2011; Lang et al. 2015). The same vestigial ligands are now evident also in the ancestral Nuo complexes of Desulfurobacteriales and Nautiliales (fig. 2*B* cf. fig. 3*A*). In particular, their NuoD proteins maintain the first and third Cys ligands of the Ni–Fe cluster, corresponding to positions 86 and 403 following *Thermus* numeration (figs. 2*B* and 3*A*). The gene sequences of ancestral forms of Nuo complexes are shown in fig. 2 and supplementary fig. S2, Supplementary Material online, which summarize information derived from the alignments of various bacterial subunits and their plastidial homologs (fig. 3*A* and data not shown).

Analysis of Nuo proteins to answer Question 1: Which are the early signatures of Q reactivity?

There is a fundamental functional difference that distinguishes *mbx* from Fpo complexes. While *mbx* and related enzyme catalyze electron transport from reduced ferredoxins to NAD(P) + (Bridger et al. 2011), Fpo complexes use as their electron acceptor a quinone analog, methanophenazine (Mph—Abken et al. 1998; Welte and Deppenmeier 2014). This is a membrane quinone chemically related to anti-microbial phenazines produced by *Pseudomonas* (Turner and Messenger 1986) and also to potent acaricide inhibitors of complex I such as fenazaquin (Hollingworth et al. 1994; Degli Esposti 1998). Hence, Fpo complexes should harbor the first set of molecular signatures enabling reactivity to membrane quinones or their antagonists along the evolution of complex I.

Sequence analysis of the NuoD subunit indicates four protein regions that contain residues forming the Q reacting chamber in *Thermus* and *Yarrowia* complex I (cf. fig. 1*A*) and are partially conserved in the homologous subunit of Fpo complexes (highlighted in black and white, fig. 3*A*). Two of these regions correspond to the ligand domains of the Ni–Fe cluster of hydrogenases and show a similar pattern of evolution. The other two regions contain the Q-binding residues H38 and D139, respectively, and follow a different pattern of amino acid variation (fig. 3*A* and table 1). Archean Fpo (Welte and Deppenmeier 2014) does have Y87, which is hydrogen-bonded to a carbonyl of Q but not H38 and D139, which are hydrogen-bonded also to each other in *Thermus* complex I (Baradaran et al. 2013). Among other residues that form part of the Q reacting chamber (fig. 1*A*), F146 and D401 appear to be already present in the NuoD homologs of *Ech* hydrogenases (fig. 3), but never together with Y87, as in Fpo complexes (table 1). Of note, substitution of one Cys ligand of the Ni–Fe cluster in *R. rubrum Ech* hydrogenase enables its reaction with quinols (Heo et al. 2002), thereby indicating a propensity for Q reactivity.

Although there appears to be no study on the reaction of bacterial or mitochondrial complex I with Mph, this compound is certainly able to accept electrons from the complex, as its midpoint redox potential (−165 mV, Welte and Depenmeier 2014) is generally higher than that of cluster N2, which reduces quinones (Sazanov 2015). Moreover, Mph is related to phenazine methosulfate, which has long been used as a redox mediator in NADH oxidation assays (Löw and Vallin 1964). The concomitant presence of Y87, F146, and D401 in the NuoD sequences of Fpo complexes (table 1) would form the minimal reaction domain for Mph and, consequently, constitute the earliest structural signature for the acquisition of Q reactivity. Indeed, these residues are not present in ancestral forms of Nuo complexes such as *mbx*, which do not use Q as an electron acceptor (table 1 and fig. 3).

To obtain independent evidence for the initial acquisition of Q reactivity in Nuo complexes, sequence analysis was next applied to the NuoB subunit binding cluster N2, which directly reduces Q (Sazanov 2015). This Fe–S cluster is unusually ligated to two consecutive cysteines in the N-terminal part of the protein (fig. 1*A*, cf. Sazanov and Hinchcliffe 2006), a feature that has been connected to the protonmotive capacity of complex I (Brandt 2006; Sazanov 2015). Alignment of the NuoB sequences indicates an abrupt appearance of this cysteine doublet in the Fpo complex of *Methanosarcina* (fig. 3*B* and table 2). Hence, the peculiar chemistry and protonmotive

Fig. 3.—Continued

inhibitor typical of each organism are listed on the right of the bottom panel, in which the blue rectangle indicates a cut of the alignment in the region not facing the Q cavity (see fig. 4*B* for the complete alignment of this part of the protein). Note that *Anaeromyxobacter* is the only genus of the Myxococcales that does not produce fruiting bodies and antimicrobial antibiotics (Huntley et al. 2011). NuoD sequences of other groups of delta proteobacteria, for instance, *Bdellovibrio* and *Geobacter*, are much closer to that of *Anaeromyxobacter* than to those of antibiotic-producing Myxococcales (their various Nuo gene clusters are reported in supplementary fig. S2, Supplementary Material online). In bold are identical or strictly conserved residues (e.g., I,L,M), whereas residues forming the Q chamber are shown in black and white following the numeration of *Thermus* subunit equivalent to NuoD (Fig. 1A, Baradaran et al. 2013). Unusual substitutions of phylogenetically conserved residues are reported in red with gray background (e.g., **N**). **D160**, residue in mature bovine 49-kDa subunit equivalent to D139 in *Thermus* that is labeled by an azido acetogenin (Masuya et al. 2014). **V** in red and yellow highlighted, mutation conferring inhibitor resistance in *Rhodobacter* (Darrouzet et al. 1988); myxothiazol, naturally occurring complex I inhibitor produced by the organism. (*B*) Alignment of the N-terminal part of NuoB/PSST subunit. The region comprises the two consecutive Cys ligands of Fe-S cluster N2 and most residues that are in the Q reacting chamber of complex I, from either *Thermus* or *Yarrowia* (highlighted in black and white). Unusual amino acid substitutions and conserved cysteines are highlighted in yellow. The organisms colored in red possess rhodoquinone. The sequence of *Chlorobium* refers to that of *Chlorobium limicola*, which is representative of NUO11 operons of green sulfur bacteria.

Table 1

Evolutionary variation of key residues of the NuoD subunit

NuoD/Nad7/49 kDa subunit Organism and enzyme complex		acceptor substrate	residues interacting with quinones - *Thermus* numbering H38	D139	Y87	T135	L138	L143	F146	R350	D401	V403	S36
Rhodospirillum rubrum	*Ech* hydrogenase	carbon monoxide	E	I	S	I	H	D	**F**	**R**	**D**	**C**	L
Thermotoga maritima	*Mbx*-like	NADP+	**H**	P	V	G	G	Y	S	R	**D**	**C**	N
Thermovibro ammonificans	**NUO11** ancestral	(NADP+)	gap	V	F	S	G	H	M	R	Y	**C**	A
Nautila profundicola	**NUO10** ancestral	(NADP+)	gap	T	F	G	G	H	M	R	H	**C**	A
Methanosarcina mazei	*Fpo*	**Mph**	P	F	**Y**	E	E	V	**F**	R	**D**	**C**	G
Ca. Methanoplasma termitum	*Fpo*-like	(MQ saturated)?	**H**	**D**	Y	A	T	**L**	**F**	R	D	**C**	M
Chlorobium	**NUO11**	**MQ(H2)**	H	D	Y	**T**	**I**	F	M	R	D	**V**	**S**
Clostridium pasteurianum	**NUO11**	**MQ**	H	D	Y	S	**L**	H	W	K	D	I	S
Paulinella chromatophora	**NDH-1**	**PQ**	H	D	Y	P	A	Q	F	K	D	I	S
Streptomyces coelicolor	**NUO14**	**MQ**	H	E	Y	T	L	S	F	K	D	V	S
Thermus termophilus	**NUO14**	**MQ (Q)**	H	D	Y	T	L	L	F	R	D	V	S
Escherichia coli	**NUO13**	**Q (MQ)**	H	D	Y	T	Q	M	V	K	E	V	S
Yarrowia lipolytica	**complex I**	**Q**	H	D	Y	S	M	L	F	K	D	V	A
Bos taurus	**complex I**	**Q**	H	D	Y	T	L	M	F	K	D	V	A

NOTE.—Residues not present in *ech* hydrogenases and acquired with Mph reactivity in Fpo complexes are in white over brown background, whereas those sporadically present in *ech* or *mbx* complexes and then acquired together with MQ(H_2) reactivity in *Chlorobi* are highlighted in light brown (cf. fig. 5). Of note, *Chlorobium* residues refer to a consensus sequence of five different species of green sulfur bacteria pivoting on *C. limicola* NUO11 (cf. fig. 3*B*).

Table 2

Evolutionary variation of key residues of the NuoB subunit

NuoB/PSST subunit Organism	enzyme complex	acceptor substrate	residues in Q reaction chamber - *Thermus* numbering C46 - N2	T40	A47	I48	M50	M51	R62	F63
Azospirillum lipoferum	*ech* hydrogenase	carbon monoxide	missing	**T**	T	gap	A	F	T	**F**
Thermotoga maritima	*mbx*-like	NADP+	missing	H	**A**	**I**	L	gap	**R**	F
Thermovibro ammonificans	**NUO11** ancestral	(NADP+)	missing	H	N	G	D	**I**	R	F
Nautila profundicola	**NUO10** ancestral	(NADP+)	missing	H	N	G	D	I	R	F
Methanosarcina mazei	**Fpo**	**Mph**	**C**	**T**	G	**V**	**M**	**I**	**R**	**F**
Chlorobium (limicola)	**NUO11**	**MQ(H2)**	**C**	S	E	G	Q	L	R	F
Clostridium pasteurianum	**NUO11**	**MQ**	**C**	T	**A**	G	M	**M**	R	T
Paulinella chromatophora	**NDH-1**	**PQ**	**C**	L	F	I	F	A	R	T
Streptomyces coelicolor	**NUO14**	**MQ**	**C**	L	A	I	M	M	R	F
Thermus termophilus	**NUO14**	**MQ (Q)**	**C**	**T**	**A**	**I**	**M**	**M**	**R**	**F**
Escherichia coli	**NUO13**	**Q (MQ)**	**C**	N	Y	V	M	V	R	F
Yarrowia lipolytica	**complex I**	**Q**	**C**	T	A	V	M	M	R	L
Bos taurus	**complex I**	**Q**	**C**	T	A	V	M	M	R	F

NOTE.—Residues not present in *ech* hydrogenases and acquired with Mph reactivity in Fpo complexes are in white over brown background, whereas those sporadically present in *ech* or *mbx* complexes and then acquired together with MQ(H_2) reactivity in *Chlorobi* are highlighted in light brown. *Chlorobium* residues refer to a consensus sequence as in table 1.

capacity associated with cluster N2 appeared early in evolution, aside if not instrumental to the acquisition of redox reactivity with the Q analog Mph (table 2). It is also present in the Fpo-like complex of *Ca. Methanoplasma termitum* (Lang et al. 2015), the NuoD homolog of which has both H38 and D139 (fig. 3 cf. Lang et al. 2015). As it is presently unknown whether *Ca. Methanoplasma termitum* contains Q analogs as in related archea (Shimada et al. 2001), its Fpo-like complex has been postulated to directly reduce disulfide reductase (Lang et al. 2015). Considering also the widespread transfer of enzymes between bacteria and archea (Nelson-Sathi et al. 2015), it remains difficult to envisage whether the Fpo-like complex of *Ca. Methanoplasma termitum* represents a truly intermediate step in the structure–function evolution of complex I. Nevertheless, the residues that concomitantly appear in the NuoD subunit of Fpo complexes (table 1) lie away from those appearing in the NuoB subunit (fig. 5).

Of note, analysis of the NuoH subunit revealed the evolutionary change of a single residue (E35, fig. 1*A* cf. fig. 4*A*) among those involved in the Q reaction chamber of *Thermus*

A NuoH/ND1

B NuoD/49kDa/Nad7

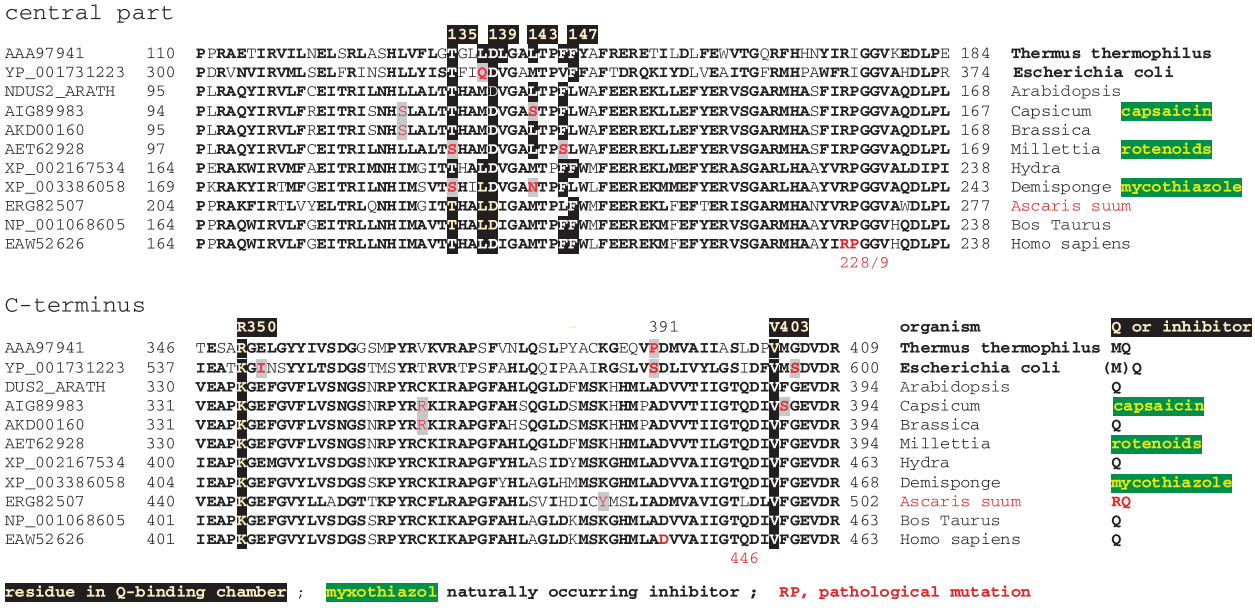

FIG. 4.—Alignment of Q-reacting subunits of complex I. (*A*) Alignment of the NuoH/ND1 subunit highlights amino acid variations related to RQ reactivity. The sequences of bacterial NuoH possessing both ubiquinone and rhodoquinone (**RQ**) such as *R.rubrum* do not show unusual amino acid substitutions in the residues that form part of the Q reacting chamber of *Thermus* complex I (in black and white) or are associated with human pathological mutations (listed in red at the bottom of the alignment, cf. Iommarini et al. 2013). However, invertebrates that have RQ (Van Hellemond et al. 1995) do show unusual substitutions at or around these residues (marked in red with gray background as in fig. 3). Most notable is the substitution of the bulky hydrophobic M42 (in *Thermus*, F in mammals) with the hydrogen-bonding S, which is shared by nematodes and the anaerobic ciliate *Nyctotherus*, which also has RQ (Müller et al. 2012). Conversely, the substitutions at position 37 and 52 appear to be restricted to nematodes, the latter being shared with bivalves such as *Mytilus*, which also have RQ (Van Hellemond et al. 1995). Bivalves additionally show nonconservative substitutions of Q43, a residue forming part of the Q reacting chamber (Baradaran et al. 2013) that is involved in pathological mutations too (Iommarini et al. 2013). See supplementary fig. S1 (Supplementary Material online) for an enlarged alignment with bacterial NuoH subunits and further information. **TM1** and *AH1*: transmembrane helix 1 and amphipatic helix AH1, respectively, in the structure of *Thermus* complex I (Baradaran et al. 2013). (*B*) Plant Nad7 and animal 49-kDa subunit show residue changes probably associated with resistance to Q antagonist inhibitors. Alignment blocks overlap and extend those of bacterial NuoD sequences in fig. 3*A* and show much stronger conservation (in bold) than across bacterial phyla. To date, only the Nad7 sequence of *Pongamia or Millettia pinnata* (accession: AET62928; Kazakoff et al. 2010) is available from the plants that produce rotenoids. It is aligned with homologous sequences from plants that do not produce rotenoids

(continued)

complex I (supplementary fig. S1, Supplementary Material online), thereby indicating that this subunit was minimally involved in the acquisition of Q reactivity by complex I.

Analysis to answer Question 2: Are natural substitutions of key residues related to different quinone types?

Following the analysis described above, the next evolutionary step in the acquisition of Q reactivity is the appearance of H38, which directly binds a Q carbonyl in *Thermus* complex I (fig. 1*A*, cf. Sazanov 2015), together with D139 (fig. 5*A* cf. fig. 1*A* and table 1). Contrary to the NuoD homologs of *Ech* hydrogenases and ancestral Nuo complexes, *Chlorobium* NuoD shows these residues concomitantly with the substitution of the first and third vestigial ligand of the Ni–Fe cluster and the appearance of phylogenetically conserved residues that lie in the vicinity of bound Q in *Thermus*, in particular T135 (figs. 3*A*, 4*B* and table 1). Such a group of structurally interconnected residues appears not only in the NUO11 complexes of *Chlorobi* but also in that of gram-positive bacteria, for instance, *Clostridium pasteurianum* (fig. 3*A* and table 1), organisms that have menaquinone (MQ) as the dominant membrane quinone. The presence of H38 and D139 in plastidial NDH-1 complexes, however, is accompanied by the substitution of T135 with Pro and other nonconservative replacements (table 3 and fig. 5*B*) that could reflect, at least in part, the adaptation to react with plastoquinone (PQ), the specific quinone of photosynthetic organisms having the NDH-1 complex (Battchikova et al. 2011). Intuitively, PQ reactivity was acquired by changing complex I residues that could accommodate the modification of the double ring of MQ into the single, di-methylated ring of PQ. These residues include strongly conserved C39 in NuoA (Zickermann et al. 2015), which is mutated to Ser in plastidial sequences (fig. 5 and data not shown), and form a concerted set of amino acid variations that is distributed across greater part of the Q reaction chamber, especially at the interface between NuoD and the other subunits of the Q module (fig. 5*B*). While accommodating the diverse quinone ring of PQ, such variations did not alter the core chemistry of Q interaction, as previously concluded for PQ-reacting cytochrome b_6 (Nelson e al. 2005).

What about complex I adaptation to naturally occurring changes in the ring substituents of Q? To provide answers to this additional question, it has been investigated whether specific variation in complex I subunits could be associated with chemically different quinones of organisms having a fully sequenced genome, starting with the archaean *Sulfolobus* that possesses very peculiar quinones such as caldarellaquinone (Shimada et al. 2001). The sequence of *Sulfolobus* NuoD does not have H38, while showing Y87 and D139 substituted with residues such as Ile, the side chain of which is unable to establish H bonds with Q carbonyls. These differences are equivalent to those observed in the NuoD sequences of Nautiliales and Desulfurobacteriales (fig. 3), suggesting a common ancestry dating before the acquisition of effective Q reactivity. The function of the Nuo complexes of these organisms presumably consists in electron transfer between ferredoxin and NADP+, as in *mbx* complexes (cf. Bridger et al. 2011; Lücker et al. 2013).

The introduction of the methoxy ring substituents that differentiate ubiquinone (Q) from MQ and PQ has occurred when oxygen levels in the environment became sufficiently high to sustain the three hydroxylation reactions required in ubiquinone biosynthesis (Aussel et al. 2014). That time corresponded with the separation of aerobic proteobacteria from other prokaryotes (Segata et al. 2013; Degli Esposti et al. 2015). In contrast with recent speculations (Welte and Deppenmeier 2014), complex I subunits of aerobic proteobacteria do not show evident sequence variation that could be correlated with Q rather than MQ reactivity (fig. 3 and results not shown). Indeed, *Thermus* complex I equally reacts with its physiological MQ substrate and DBQ (Baradaran et al. 2013). However, peculiar changes have been noted in both the NuoD and the NuoH sequences of organisms that possess the rare Q analog, rhodoquinone (2-methoxy,3-amino,5-methyl,6-isoprenyl,2-4*p*-benzoquinone, RQ; figs. 4 and 5; table 3).

The replacement of one methoxy substituent with an amine group in RQ increases the number of potential H bonds that can be formed with interacting proteins. Hence, additional residues forming H bonds are in principle required for adapting Q-reacting enzymes to RQ, which normally is a poor substrate for respiratory complex I and II (Lenaz et al. 1968). Among bacteria, only *R. rubrum* and *R. photometricum* possess high levels of RQ (Hiraishi and Hoshino 1984). Conversely, RQ distribution is relatively dispersed among protists and metazoans adapted to anaerobiosis, such as the nematode *Ascaris* and the ciliate *Nyctotherus,* which contain RQ in their anaerobic mitochondria (Müller et al. 2012). Fortunately, there is a valuable model to discern RQ-specific changes, the Q-reducing **Qi** site in cytochrome *b* of the

Fig. 4.—Continued

(*Arabidopsis* and *Brassica*) as well as *Capsicum*, which produces the weak complex I inhibitor capsaicin (Shimomura et al. 1989; Degli Esposti 1998). Of note, the sequence of *Capsicum* is very similar to that of other members of the *Solanoideae* family for which natural resistance to rotenoids has been documented, for example, potato. The sequence of the 49-kDa subunit of *Amphymedon queenslandica* (Srivastava et al. 2011) is aligned together with plant Nad7 and animal homologs to represent the protein variation in demisponges, which produce the complex I inhibitor mycothiazole (Morgan et al. 2010). Unusual or nonconservative substitutions are in red over gray background as in figs. 3, whereas sites of human mutations are in dark red as in *A*.

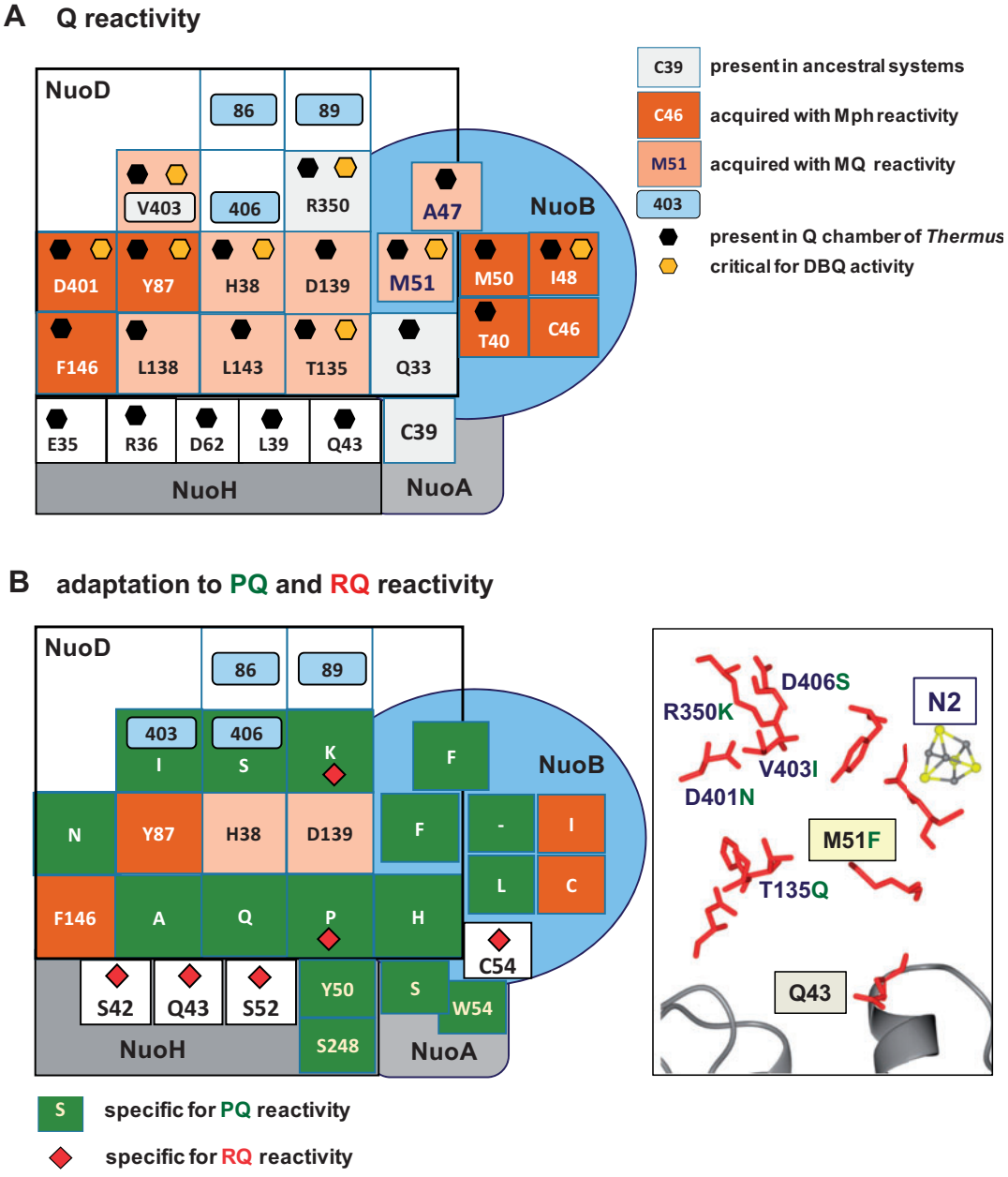

FIG. 5.—Model for progressive acquisition of Q reactivity by complex I. (*A*) Evolution of the reactivity with quinones. The 5 × 4 matrix represents the set of NuoD residues forming the Q reaction chamber in the crystal structure of complex I (fig. 1*A*, cf. Baradaran et al. 2013); on the right, it is shown empty and overlapped by residue M51 of the NuoB subunit to emphasize the closeness of the latter subunit in the 3D structure of *Yarrowia* complex I (Zickermann et al. 2015). The interaction of NuoD with the other Q-reacting subunits, transmembrane NuoH and NuoA, is modeled taking into consideration the membrane topology of the proteins (fig. 1*A*) and the overall distribution of inhibitor-resistant sites (table 3). Residues colored in dark brown are present in *Ech* hydrogenases or have been acquired with Mph reactivity in Fpo complexes, whereas those colored in light brown have been acquired with the reactivity with MQ in the NUO11 of *Chlorobi* and other bacteria (tables 1 and 2). Black hexagons indicate the residues forming the Q reaction chamber in *Thermus* complex I (Baradaran et al. 2013). Of these, only F147 and S36 of the NuoD subunit are not shown in the scheme; anyway, table 1 reports the evolutionary variation of S36. The yellow hexagons indicate the residues that show about 80% reduction in the NADH-DBQ activity of either *Yarrowia* (Tocilescu et al. 2007, 2010b) or *E. coli* complex I (Baradaran et al. 2013; Sinha et al. 2015). (*B*) Amino acid variation following chemical changes in natural quinone acceptors. The green squares indicate changes in Q-binding residues of complex I subunits that are potentially related to the reactivity toward PQ (table 3). The panel on the right, derived from the 3D images in fig. 1*A*, shows the principal Q-reacting residues of the NuoD and NuoB subunits as red cylinders; those that are changed in PQ-reacting complex I are indicated to provide structural reference to their position in the scheme on the left. Red diamonds indicate sites showing unusual amino acid changes that are present in the sequences of organisms having the natural Q analog, rhodoquinone (RQ, cf. fig. 4 and table 3).

Table 3

Amino acid variations in complex I subunits associated with Q function and resistance to Q antagonist inhibitors

A	B	C	D	E	F	G	H	I	J	K	L	M
	Table 3											
							Q antagonist inhibitor resistance (to, induced)					
Subunit organism	residue & position *Thermus* number	Q pocket *Thermus*	*E.coli* & NUO13	PQ plastid NDH-1	RQ	DBQ activity	piericidin A *Streptomyces*	rotenoids Papilionoideae plants	DQA & other quinazolines	myxococcal antibiotics	capsaicin Solanoideae plants	mycothiazole Demisponges
NuoA/ND3	C39		S	S						A		
	K48			W								
NuoB/PSST	T40	yes	N	L						P		M (Cnidaria) g
	C45	NiFe ligand										
	C46	NiFe ligand										
	A47	yes	Y	F				Y		G		G (Cnidaria) g
	I48	yes							to M - resistant			
	E49									Y		
	M50	yes		DELetion								
	M51	yes		F				to C- resistant	to C- resistant			
	S54				C							
NuoH/ND1	E35	yes					to Q - resistant			to Q - resistant e		
	R36	yes					H					
	R37											
	L39	yes		S								
	F(M)42				S				?			
	Q43	yes			G,M							
	(R)V50			Y			Y			INsert		
	G52				S				?	INsert		
	Q58									H		
	D62	yes										
	A63							to T - pathological and resistant				
	E248			S								
NuoD/Nad7 /49 kDa	Q33	yes	N	H						S		
	H38	yes							to R - resistant			
	G39								to A - resistant		to A - resistant	
	R84							to K - resistant	to K - resistant			
	M85			W			H					
	D86	NiFe ligand	E					to A - resistant	to A, C - resistant	N		
	Y87	yes					W to W, F - resistant	to W, F - resistant	to F - resistant		to F - resistant	
	H89	NiFe ligand						to C, V - resistant	to C, V - resistant			
	T135	yes		P	S a		S	S d		A		S
	L138	yes	Q	A				Q	Q			
	D139	yes					*		*		to A - resistant	
	L143	yes		Q							S	N
	F146	yes						S , to E - resistant	to E - resistant			
	V150							to H - resistant	to H - resistant		to H -resistant f	
	R350	yes			T a		L		K to R - resistant	N		
	D392											
	D401						F to A - resistant	to A - resistant	to A - resistant	N		
	V403	NiFe ligand					to M - resistant	to L- resistant	to L- resistant			
	M404							S		G	S	
	G405						to A - resistant c					
	D406	NiFe ligand		S					to Q - resistant			
	D408						to E- resistant c	to E- resistant				
	R409									Q		
					a bacteria	mitos or *E.coli*	c also to Pyridaben	d S to T in *Yarrowia*, increased sensitivity	? hypersensitivity in *Ascaris*	e stigmatellin in *E.coli*	f C12E8 in *Yarrowia*	g available genomes

NOTE.—Inhibitors are naturally occurring (their natural origin is annotated in the first row of the table), with the exception of quinazolines, for example, DQA. These synthetic inhibitors have been included given the abundance of mutagenesis data (Yamashita et al. 2004; Fendel et al. 2008; Murai et al. 2009; Tocilescu et al. 2010b; Sinha et al. 2015) and their resemblance to methanophenazine (Mph), the natural acceptor substrate for Fpo (Abken et al. 1998). Red squares in the central column indicate residues associated with approximately 80% reduction in DBQ activity after mutation (Tocilescu et al. 2007; Sinha et al. 2015). The question mark under the column of quinazoline inhibitors indicates possible hypersensitivity in *Ascaris* vs. bovine (Yamashita et al. 2004), whereas that in the column of mycothiazole indicates possible variations deduced from the available sequence of Cnidaria (see text). The asterisk under the columns of piericidin and quinazoline inhibitors indicates the labeling of the equivalent bovine residue with an acetogenin analog that can be displaced by bullatacin and quinazoline inhibitors (Masuya et al. 2014).

cytochrome bc_1 complex, which is functionally equivalent to the Q-reducing site in complex I. Cytochrome *b* proteins that exclusively react with Q show a notable amino acid variation at the **Qi** site with respect to cytochrome *b* proteins that react with either MQ or PQ (supplementary fig. S3, Supplementary Material online): the substitution of the bulky hydrophobic Ile with Ser at position 206 (yeast numbering; Degli Esposti et al. 1993a). S206 is indeed H-bonded to one methoxy group of bound ubiquinone in crystal structures of the bc_1 complex (Berry et al. 1999; Gao et al. 2003; Schütz et al. 2003). Additionally, the cytochrome *b* of RQ-containing organisms that retain also Q in their membranes, such as *Rhodospirillum* and *Mytilus*, shows the substitution of the nearby residue Thr204 with Lys, a change that also increases the capacity of forming H bonds (supplementary fig. S3, Supplementary Material online). In the aligned sequences of the NUOH/ND1 subunit of complex I, a substitution equivalent to that at position 206 of cytochrome *b* is observed at position 42, where bulky hydrophobic residues (Met in mammals or Phe in *Thermus*) are substituted by Ser in *Nyctotherus* and nematodes, but not other invertebrates (fig. 4*A*). The same organisms, together with those experiencing recurrent cycles of anaerobiosis like *Mytilus*, also show the substitution of conserved G52 with H bond-forming Ser or Thr (fig. 4*A*).

Moreover, ND sequences from bivalves show nonconservative substitutions of Q43, which is part of the Q reacting chamber in *Thermus* (fig. 1*A* cf. fig. 4*A*). Position 43 and 52 are associated with pathological mutations too (fig. 4*A*, cf. Iommarini et al. 2013).

All the above changes in the ND1 subunit do not occur in the homologous NuoH subunit of RQ-containing *Rhodospirilli*, which instead show specific replacement of two Q-interacting residues in NuoD (fig. 3*A* and supplementary fig. S1, Supplementary Material online) and one in NuoB (table 3). Hence, complex I adaptation to RQ reactivity has followed different evolutionary paths in proteobacteria and mitochondria. Consequently, the sporadic presence of RQ in eukaryotes cannot be considered a *bona fide* relic from the bacterial ancestors of mitochondria (see Müller et al. 2012 and discussion therein), otherwise complex I adaptation to react with RQ would have involved the same subunits in prokaryotes and eukaryotes.

Answer to Question 3: Complex I changes in organisms producing Q antagonist inhibitors

After obtaining insights on Q reactivity and its adaptation to diverse natural Q substrates, the analysis was extended to the Nuo subunits of organisms that produce Q antagonist inhibitors of complex I (figs. 3*A* and 4*B*). Such organisms must have adapted their Q reaction sites so as to minimize the inhibitory action of the Q antagonists they produce, in analogy with earlier studies on natural resistance toward Q antagonist inhibitors of the bc_1 complex (Ghelli et al. 1992; Degli Esposti et al. 1993a; Kraiczy et al. 1996; Ouchane et al. 2002). The most potent inhibitors of complex I derive from plants of the *Annonaceae* family, for example, rolliniastatin-2 or bullatacin (Degli Esposti 1998); however, no full sequence of complex I subunits from *Annonaceae* is available to date. Labeling studies in bovine heart mitochondria have indicated that these acetogenins interact with both the ND1 and the 49-kDa subunits of complex I (Masuya et al. 2014). In the latter protein, an acetogenin analog specifically binds to the residue corresponding to D139 in *Thermus* complex I (fig. 3*A*); this binding is displaced not only by bullatacin, but also by a quinazoline inhibitor (Masuya et al. 2014).

Piericidin A is next in potency to acetogenins and is produced by organisms of the *Streptomyces* group of gram-positive bacteria (Takahashi et al. 1965; Chen et al. 2014). The genome of some piericidin-producing *Streptomyces* strains is currently available and codes for early versions of NUO14 complexes that are expressed in the normal physiology of the bacteria (Surup et al. 2008; Spero et al. 2015). The NuoD and NuoH subunits of these piericidin-producing organisms show remarkable substitutions of amino acids forming the Q reaction chamber in *Thermus* complex I (table 3), even in comparison with closely related species that produce weak complex I inhibitors such as iromycins (Surup et al. 2008), which have NuoD sequences very close to that of *S. coelicolor* (Borodina et al. 2005), shown in fig. 3. These substitutions are either unique or very rare and isolated among the numerous sequences from *Streptomyces* and other Actinomycetes that are now available, thereby defining likely correlations with natural resistance toward piericidin inhibitors. In particular, piericidin-producing strains show the substitution of Y87 with Trp (W, fig. 3*A* and table 3), an identical change to site-directed mutations that produce severe reduction in DBQ activity and strong resistance to rotenone and other complex I inhibitors (Kashani-Poor et al. 2001; Tocilescu et al. 2010b; Sinha et al. 2015). Another remarkable change occurs at position 401 of NuoD, the same site that was previously found to be responsible for resistance to piericidin A in *Rhodobacter* mutants (Darrouzet et al. 1998; table 3). These and other sites of experimentally induced or natural resistance toward piericidin A have been mapped in the diagram containing the residues forming the Q reaction chamber in *Thermus* complex I (fig. 6, cf. figs. 1*A* and 5). Their distribution appears to define two domains (fig. 6), consistent with earlier evidence that piericidin A binds to two sites in complex I (Gutman et al. 1970; reviewed by Degli Esposti 1998). The first domain is formed by three residues of the NuoH subunit (E35, R36, and R50) and several residues of the NuoD subunit that are either involved in the binding of piericidin A in the crystal structure of *Thermus* (Baradaran et al. 2013) or lie near the Q reaction chamber, such as M85 and G405 (fig. 1*A* cf. fig. 6). The second domain includes a few NuoD residues, in particular T135 and R350, which are also linked to natural resistance toward myxococcal antibiotics (fig. 6 and table 3).

Myxococcal antibiotics include potent Q-antagonist inhibitors of bacterial and mitochondrial respiratory chains that are produced by predatory delta proteobacteria of the order Myxococcales, for example, *Myxococcus* and *Stigmatella* (Reichenbach et al. 1988; Friedrich et al. 1994; Degli Esposti 1998). Among these Q-antagonists, myxothiazol and stigmatellin inhibit both the bc_1 complex and complex I (Degli Esposti et al. 1993a; Degli Esposti 1998) and are produced in mixtures that vary between species and strains (Reichenbach et al. 1988). *Anaeromyxobacter* is a clear exception among Myxococcales because it does not produce the fruiting bodies in which the antibiotics are stored (Huntley et al. 2011). Consequently, the sequences of complex I subunits of *Anaeromyxobacter* can be used as a reference for identifying unusual amino acid changes that may confer resistance to myxococcal Q-antagonist inhibitors. These changes occur at several NuoD sites (H38 to S, D86 to N, T135 to A, R350 and D401 to N) that form part of the Q reacting chamber in *Thermus* complex I (table 3, figs. 3 and 6, cf. fig. 1*A*). The same changes are present in the NuoD sequence of *Sorangium* (fig. 3), a close relative of the *Polyangium* strains that produce phenoxan—the most potent inhibitor of complex I among myxococcal antibiotics (Kunze et al. 1992; Friedrich et al. 1994)—for which no Nuo gene is currently

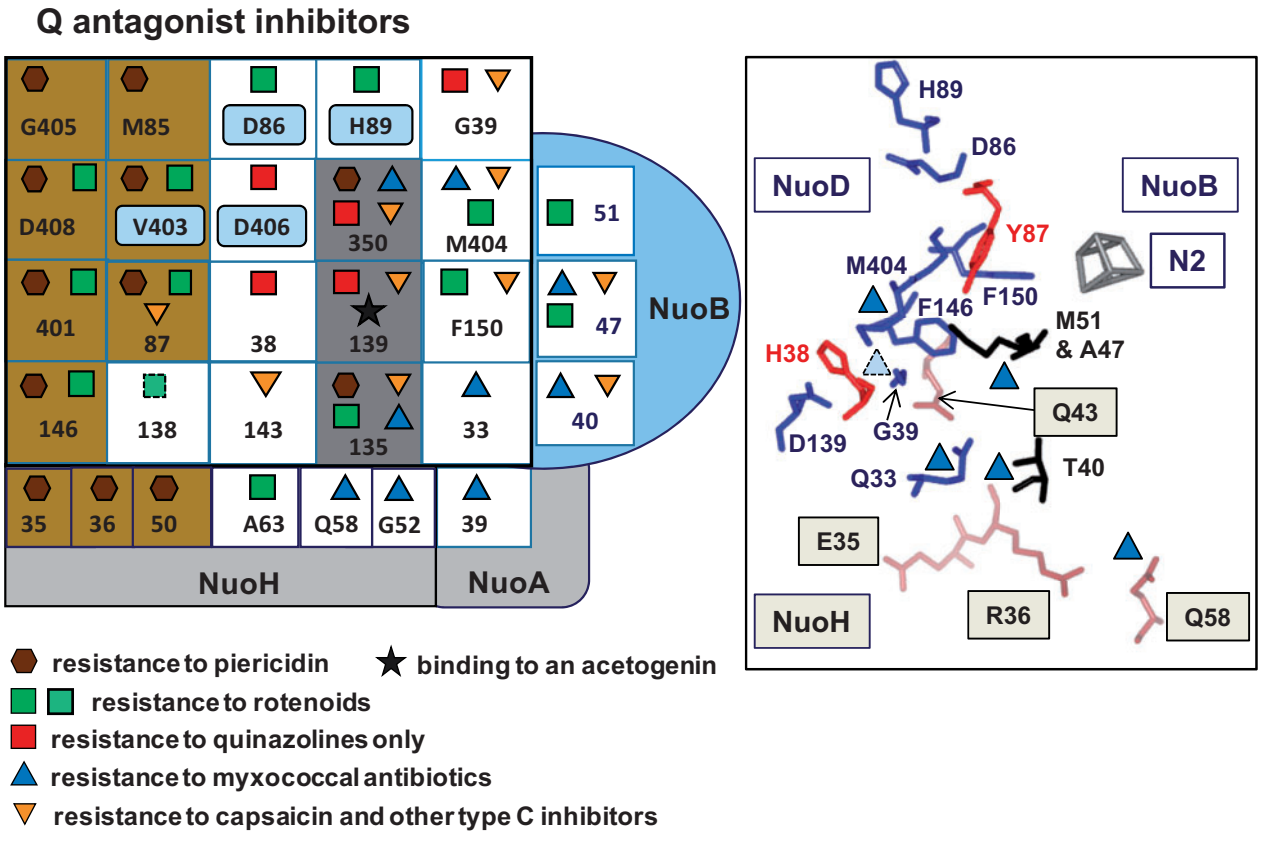

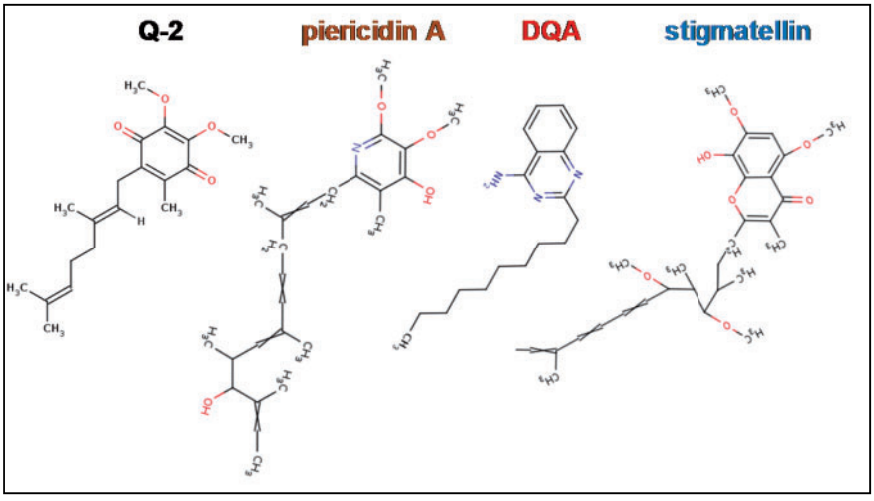

Fig. 6.—Mapping Q-antagonist inhibitors around the Q reaction chamber of complex I. The residues associated with resistance toward naturally occurring and quinazoline inhibitors of complex I (table 3) are mapped on the model representing the Q-reacting subunits (fig. 1*A*), modified from that presented in fig. 5 in the overlapping of M51 of the NuoB subunit over the NuoD subunit to introduce two additional residues of the latter protein, M404 and G39. Although not listed among the Q-interacting sites by Baradaran et al (2013), these residues form part of the Q cavity in the crystal structure of *Thermus* complex I (see right panel) and are associated with resistance to Q antagonist inhibitors (table 3). Moreover, M404 has been found crucial for DBQ activity (table 3, cf. Tocilescu et al. 2007; Fendel et al. 2008). Graphical symbols indicate inhibitor resistance—either natural or experimentally induced by mutagenesis—as follows: brown hexagons, piericidin A as in fig. 1*A*; green squares, rotenoids; light green square, deduced rotenone resistance in *E. coli* (Friedrich et al. 1994); red squares, DQA and other quinazoline inhibitors without cross-resistance to rotenone (cf. Fendel et al. 2008); blue triangle, myxococcal antibiotics (e.g., myxothiazol and stigmatellin); orange inverted triangles, capsaicin and other type C inhibitors such as C12E8 (cf. Tocilescu et al. 2010b); gray star, position binding an acetogenin analog that is displaced by bullatacin and quinazoline inhibitors (Masuya et al. 2014). The sponge-produced

(continued)

available. It thus appears that complex I of delta proteobacteria has adapted to counteract all myxococcal Q antagonists by a common set of residue substitutions that are spread across the NuoD and NuoB subunits forming the Q reaction chamber (table 3, figs. 3 and 6). Moreover, the NuoA subunit of Q-antagonist-producing Myxococcales shows the substitution of the highly conserved C39 with Ala (table 3, cf. Zickermann et al. 2015), while recurrently replacing highly conserved Asp residues with Asn in the NuoD subunit (fig. 3 and table 3). Interestingly, natural resistance to myxococcal antibiotics involves sites that are also changed in PQ-reacting proteins (fig. 6*B* cf. fig. 5*B*), or are associated with resistance toward rotenone and quinazoline inhibitors (table 3). Hence, complex I evolution could have followed a common structural strategy to reduce the interference of Q antagonist inhibitors and adapt its reactivity to Q substrates different than MQ, which is the standard quinone in delta proteobacteria (Iizuka et al. 2003).

Other naturally occurring Q antagonists include rotenone, the classical inhibitor of complex I (Singer and Ramsay 1994; Degli Esposti 1998). Rotenone is part of the isoflavonoid family of rotenoids produced by *Derris* and *Millettia*, leguminosae plants that belong to the *Millettiae* tribe (Brierley and Smith 1968; Simin et al. 2002; Ngandeu et al. 2008). Among the species producing rotenoids, only the Nad7 sequence of *Millettia pinnata* is currently available (Kazakoff et al. 2012) and its alignment with homologous sequences from plants that do not produce rotenoids (e.g., *Arabidopsis*) indicate the substitution of two residues that form part of the Q reaction chamber in complex I: T135 and F146, both changed to Ser (fig. 4*B* cf. fig. 3). The first substitution is the opposite to a directed mutation introduced in the homologous 49-kDa subunit of *Yarrowia*, which also has Ser at position 135 and is naturally resistant to rotenone (Fendel et al. 2008; Tocilescu et al. 2010b). Re-introduction of T135 is associated with an increased sensitivity toward rotenone in *Yarrowia* complex I (Fendel et al. 2008), thereby validating the possibility that its replacement with Ser in some plants confers natural resistance toward rotenoids. This substitution remains unique to rotenone-producing *Millettia* when combined with the substitution of F146 with Ser (fig. 4*B* cf. fig. 3). Conversely, Nad7 sequences of *Solanoideae* plants show the rare substitution of both L143 and M404 (Phe in other eukaryotes) with Ser (fig. 4*B*). Among these plants is *Capsicum*, which produces the weak complex I inhibitor capsaicin (Shimomura et al. 1989), as well as potato. Hence, the changes of either L143 or M404 could be associated with natural resistance toward capsaicin and may also be responsible for the strong rotenone resistance documented in potato complex I (Degli Esposti 1998). Of note, a substitution of position 404 with Ser in NuoD has been found to be responsible for *in vivo* resistance of *Helicobacter* strains to benzimidazole inhibitors (Mills et al. 2004), compounds that belong to type C inhibitors (Andreani et al. 1995; Degli Esposti 1998). Recently, rotenone has been reported to inhibit also the ferredoxin-mediated NADPH oxidase activity of the NDH-1 complex isolated from the cyanobacterium, *Thermosynechococcus elongatus* (Hu et al. 2013). The NuoD homolog of this complex has the same variations in the Q reacting chamber as those present in the related *Synechocystis* shown in fig. 3*A*. As only two of such variations occur at sites associated with rotenone resistance (table 3), rotenone sensitivity of cyanobacterial NDH-1 complex fits with the structure–function relationships deduced here.

Mycothiazole is a novel complex I inhibitor that has been recently isolated from marine demisponges, for which only the sequence of the 49-kDa subunit of *Amphymedon queenslandica* is currently available (Srivastava et al. 2011). Its alignment with NuoD homologs shows the substitution of T135 with Ser combined with that of L143 with Asn (figs. 3 and 4*B*). The combined changes are similar to those found in *Millettia* but include a different hydrophobic residue forming the Q reaction chamber, namely, L143 instead of F146. However, both residues lie in the vicinity of bound ubiquinone (figs. 1*A* and 6, cf. Fendel et al. 2008) and therefore could contribute to the binding of either rotenone or mycothiazole, as well as capsaicin (see above). This possibility would imply that mycothiazole may function like rotenone in inhibiting complex I, a possibility that is consistent with some biochemical data (Morgan et al. 2010 cf. Degli Esposti 1998), but needs to be substantiated by detailed studies on complex I of demisponges. In the meantime, complex I sequences available from marine metazoans, such as the cnidarian *Nematostella* (Putnam et al. 2007), show

Fig. 6.—Continued

mycothiazole is tentatively considered to overlap both rotenone and type C inhibitors (table 3). The residues associated with resistance towardsthe first site of piericidin interaction are highlighted in light brown (left), whereas those that may form the second piericidin site are highlighted in gray (within NuoD only, right). Contrary to this second site, the first piericidin site is separated from the distribution of the residues associated with resistance toward myxococcal antibiotics. Note that the sites associated with rotenone and quinazoline resistance accumulate in the central part of the diagram, overlapping the resistance sites for both piericidin and myxococcal antibiotics. The panel on the right shows a 3D image of the Q reaction chamber of *Thermus* complex I as presented in fig. 1*A*, but with a downward tilt to better visualize the position of many residues presented in the scheme on the left. H38 and Y87 binding to Q are colored in red, whereas other residues of the same NuoD subunit are in blue, as in fig. 1*A*. Conversely, residues involved in inhibitor resistance that belong to the NuoB and NuoH subunit are colored in black and tan, respectively. Blue triangles indicate residues involved in the resistance to myxococcal antibiotics, as in the scheme of the left panel. The pale blue dashed triangle indicates the position of T135, which is not shown for sake of clarity. The chemical structures of piericidin A, DQA, and stigmatellin—a representative of myxococcal antibiotics—are shown in the bottom panel and compared with that of Q-2.

changes in the Q-interacting residues of the NuoB subunit (reported in table 3 too), which perhaps reflect instances of natural resistance toward mycothiazole and other natural complex I inhibitors released in the ocean, an area or biological research that has yet to be explored.

Rotenone resistance in NUO13 complex I and its evolutionary implications

NUO13 Complex I of *E. coli* is known to be strongly resistant to rotenone (Friedrich et al. 1994), contrary to the NUO14 complex I of other proteobacteria such as *Paracoccus* or *Rhodobacter capsulatus* (Darrouzet et al. 1998; Dupuis et al. 1998). The analysis just presented suggests the first molecular reasons to explain *E. coli* resistance to rotenone (table 3). Across all Q-reacting subunits of complex I, *E. coli* sequences show six amino acid replacements that occur at the same sites that are modified in PQ-reacting plastidial subunits, including Cys39 to Ser in NuoA (table 3). In NuoD, the replacement of Q-interacting L138 with Q (fig. 4*B*) is similar to mutations induced in nearby sites producing resistance to rotenone and DQA in *Yarrowia* complex I (Tocilescu et al. 2010a, b) and therefore is likely to contribute to rotenone resistance in *E. coli* (table 3). Four sites that are unusually substituted in *E. coli* NuoB and NuodD are also changed in Myxococcales (table 3), in agreement with the resistance of *E. coli* complex I to myxococcal inhibitors too (Friedrich et al. 1994). Conversely, *E. coli* NuoD shows only the nonconservative substitution of M85 among the sites that could be associated with natural resistance to piericidin (table 3, cf. fig. 1*A*). This observation is consistent with the moderate sensitivity of *E. coli* complex I to piericidin A (Friedrich et al. 1994) compared with other proteobacteria (Grivennikova et al. 2003). Interestingly, the changes observed in *E. coli* subunits are also seen in the NUO13 complex of other species that either have only this type of complex I (e.g., *Asaia*) or additionally have a NUO14 complex I, as in *Rhodopseudomonas palustris* (Oda et al. 2008; Spero et al. 2015). It is not clear why some organisms possess two different types of complex I. NUO13 complexes may be predominantly involved under anaerobic conditions (Spero et al. 2015), or in reverse electron transport to supply NADPH for biosynthetic purposes (Sharma et al. 2012; Lücker et al. 2013). However, the NUO14 complex of *Rhodobacter* is considered to predominantly work in reverse electron transport (Dupuis et al. 1998; Herter et al. 1998).

The present work suggests another explanation for the presence of different Nuo operons in some bacteria, which is based on the spectrum of amino acid changes associated with resistance toward naturally occurring inhibitors (table 3). The NUO13 complex may confer ecological (and consequently also evolutionary) advantages in environments where predatory Myxococcales thrive, for example, soil, because it can provide bioenergy and metabolic activities that remain insensitive to the Q antagonist antibiotics released by competing myxococcal organisms. Indeed, the presence of both NUO13 and NUO14 complex I is common among soil bacteria such as *Rhodopseudomonas*, which require complex I function in their metabolic adaptation to changes in soil environments (Oda et al. 2008; Spero et al. 2015). Although it has been assumed that myxococcal antibiotics are released to successfully compete with protists and fungi in the soil (Reichenbach et al. 1988), it is plausible that some bacteria might have evolved successful strategies to counteract the same antibiotics.

Functional studies with Q substrates re-define the old concept of two Q reaction sites in complex I

The structural deductions presented so far could be correlated with a wealth of biochemical data that suggested two different Q or inhibitor sites in complex I, an old concept in bioenergetics (Gutman et al. 1970; Singer and Ramsay 1994). Differences in complex I reaction with Q can be discerned by using protonmotive measurements with chemically diverse quinones, as the initial reduction and subsequent protonation of Q substrates contribute differently to the proton pumping capacity of the complex (Degli Esposti et al. 1996; Helfenbaum et al. 1997; Ohshima et al. 1998; Sharma et al. 2015). The bioenergetic capacity of natural Q analogs discussed here and of other quinones is compared in fig. 7 and the results, together with previous reports (Degli Esposti et al. 1996; Helfenbaum et al. 1997), operationally define two Q reaction sites in complex I: the distal, hydrophobic site where the Q substrates enter the complex and are initially reduced—in a reaction intensely coupled to protonmotive activity—and the hydrophilic site where the reduced substrates then move, before being released as products. The latter site produces little membrane potential and is most accessible to hydrophilic quinones such as Q0 (2,3-dimethoxy,5-methyl,*p*-benzoquinone, cf. Degli Esposti et al. 1996).

The relative efficiency in membrane potential generation decreases in the order of decyl Q, PQ, and RQ, despite the similar hydrophobicity of these analogs; the rates of decyl RQ are even lower than those of Q0 (fig. 7*A*). All these quinones generate membrane potential when equilibrated with mitochondrial particles before the addition of NADH to initiate the reaction (fig. 7*A*). However, when they are added after the particles have been equilibrated with NADH, only DBQ and Q-1 produce similar rates of membrane potential generation (fig. 7*B*). In contrast, PQ, RQ, and Q0 produce hardly any membrane potential under these conditions leading to full reduction of endogenous Q, even if they still function as electron acceptors for the redox reaction of complex I (not shown; cf. Lenaz et al. 1968; Ruzicka and Crane 1970; Degli Esposti et al. 1996; Fato et al. 1996; Ohshima et al. 1998). This remarkable difference in membrane potential generation whether the reaction is started with NADH or Q is simply explained by considering that endogenous QH_2 occupies the hydrophilic

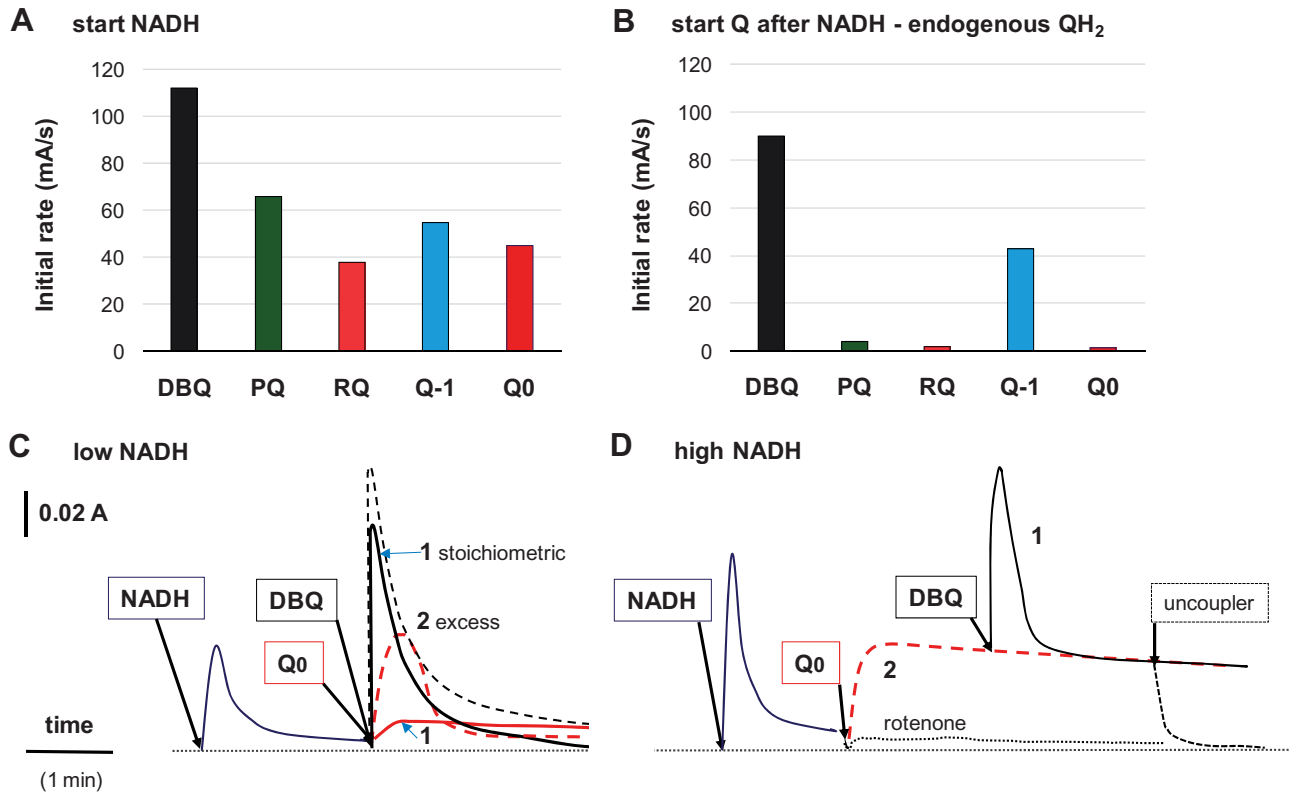

Fig. 7.—Membrane potential generation in bovine complex I with different Q analogs. Generation of membrane potential by complex I was measured by following the absorbance changes of oxonol VI in coupled submitochondrial particles from bovine heart (to a final concentration of 0.15-0.2 mg/ml) activated with NADH and then treated with inhibitors of other respiratory complexes plus nigericin as described earlier (Degli Esposti et al. 1996; Helfelbaum et al. 1997). PQ and RQ refer to the decyl analog of PQ and rhodoquinone, respectively. (*A*) The reaction was started with 0.1 mM NADH after the quinones had been equilibrated at a final concentration of *ca.* 0.02 mM for at least 2 min with the particles. (*B*) The reaction was started with *ca.* 0.02 mM quinone after the particles had been equilibrated with 0.1 mM NADH for at least 2 min. (*C*) Reproduction of the absorbance recording at 630 minus 601 nm obtained with a Cary spectrophotometer using the conditions described by Degli Esposti et al. (1996) with only 5 μM NADH, which enabled approximately one-half the membrane potential burst obtained with saturating concentrations of NADH (cf. *D*). Subsequent addition of a stoichiometric (**1**) concentration of Q elicited very different levels of membrane potential for Q0 (red solid trace) and DBQ (black solid trace). The dashed lines represent instead the traces obtained with the addition of excess (**2**, 0.02 mM) of either quinone. (*D*) The experimental conditions were as in *C* but the concentration of NADH was 0.1 mM, close to the saturation level for reducing complex I. After the initial addition of excess Q0 (0.02 mM as in *C*), in-flight addition of 5 μM DBQ produced rapid generation of membrane potential that followed a very similar time-course to that obtained in the absence of Q0 (cf. *C*). After this was completed, complex I maintained the slowly decaying level of membrane potential generated by Q0 alone, which proceeded until complete exhaustion of excess reductant, as described earlier (Helfenbaum et al. 1997). On the right, such a reaction was interrupted by the addition of the uncoupler CCCP (0.5 μM). The dotted line at the bottom represents the trace obtained on the addition of excess Q0 after the particles had been treated with 0.3 μM rotenone, showing essentially complete inhibition of membrane potential generation. Under the same conditions, a small generation of membrane potential was observed with DBQ (Degli Esposti et al. 1994). The results are representative of three to four similar experiments conducted in part by collaboration with Anna Ghelli and Bruna Benelli (University of Bologna).

site in the complex pre-reduced with NADH and effectively competes with hydrophilic Q0, as well as PQ and RQ, but not with DBQ. Complex I has a much higher affinity for oxidized than reduced Q (Verkhovsky et al. 2012) and this applies also to hydrophobic Q analogs having 9 to 11 carbons in their tail (Degli Esposti et al. 1996); hence, endogenous QH_2 does not compete with these quinones.

The above explanation is consistent with structural data, as hydrophilic quinones and ring-substituted Q analogs such as PQ, once penetrated inside the Q reaction chamber through the common entry, would preferentially react with the amino acids that normally interact with QH_2, which minimally contribute to membrane potential generation in complex I (Degli Esposti et al. 1996; Helfenbaum et al. 1997). Among the quinones shown in fig. 7, only Q-1 interacts with both the distal and the hydrophilic site, especially in the absence of endogenous QH_2; the same would apply to Q-2, which is small enough to elicit double occupancy of the Q reaction chamber, but is more efficient than Q-1 in displacing endogenous QH_2 owing to its increased hydrophobicity (Degli Esposti et al.

1996). Structurally similar to Q-2, piericidin A (cf. fig. 6) would occupy the two sites simultaneously, for it appears to have similar affinity for either site (Gutman et al. 1970).

This rationalization of the differential functional activity of various Q analogs implies that hydrophilic Q0 would not enter the distal site, whereas DBQ would react with the same site even in the presence of excess Q0 (or quinols) at the hydrophilic site. The results presented in fig. 7 sustain this possibility, as they show the additive effect of DBQ (at low concentrations, equivalent to those of NADH in fig. 7*C*) in generating membrane potential following excess of Q0 (fig. 7*D*). The transient trace of additional membrane potential has the same time-course and similar intensity as that produced by DBQ in the absence of Q0 (fig. 7*C* and *D*). Of note, rapid addition of excess Q0 during DBQ-induced membrane potential had little effect on the recorded absorbance changes. Consequently, DBQ generates membrane potential that is additive to the rotenone-sensitive potential generated by Q0, thereby indicating two Q reaction sites. Indeed, DBQ produces equimolar oxidation of NADH, whereas Q0 induces over-stoichiometric oxidation of NADH until complete exhaustion of the reductant, as also indicated by the trace obtained with excess Q0 in fig 7*C* (trace 2). The latter effect is owing to the electron sink capacity of hydrophilic quinones including Q-2 that elicit double occupancy and reciprocal dismutation within complex I (Degli Esposti et al. 1996; Helfenbaum et al. 1997).

Conclusions

This work has exploited the abundant genomic information available today to obtain new insights into the evolution of the structure and function of respiratory complex I, an ancient bioenergetic enzyme. The in-depth analysis of catalytic protein subunits helps re-defining the concept that respiratory complex I may contain two sites of interaction with Q substrates or their antagonists, which generated a long-standing debate in bioenergetics after the detailed biochemical studies of T. Singer and co-workers (Gutman et al. 1970; Singer and Ramsay 1994). Subsequent studies with various inhibitors of complex I (Friedrich et al. 1994; Degli Esposti et al. 1994; Degli Esposti 1998) converged with biophysical studies on semiquinones (Magnitsky et al. 2002) and photoaffinity labeling experiments (Schuler et al. 1999; Murai et al. 2009) in sustaining the presence of two Q or inhibitor sites in complex I. In contrast, U. Brandt and co-workers have considered all the above evidence to be compatible with a single large cavity for Q and inhibitors in complex I, predominantly on the basis of binding (Okun et al. 1999) and mutagenesis results (Brandt 2006; Fendel et al. 2008; Tocilescu et al. 2010b). The concept of a single Q or inhibitor site was later sustained by the structural work by A. Sazanov and co-workers, who showed an unusually large Q reacting chamber in *Thermus* complex I, into which a single molecule of either DBQ or its antagonist piericidin A was bound (Baradaran et al. 2013). However, the structure of *Yarrowia* complex I (Zickermann et al. 2015) shows that the Q-antagonist DQA is bound to a restricted pocket corresponding only in part with that binding Q in *Thermus* complex I (fig. 1*A*, cf. Sazanov 2015). This structural difference has inspired the present work.

In evolutionary stages, structurally different parts of the vast Q reaction chamber (fig. 1*A* cf. Sazanov 2015) were formed at the time in which complex I acquired reactivity with the quinone analog, Mph, which is rather similar to Q antagonist inhibitors such as quinazolines (tables 1 and 2 and fig. 5). The distal Q site was initially restricted to the NuoD subunit and later incorporated the extrinsic loop following the first transmembrane helix of the NuoH subunit, which frames the Q entry into the complex (figs. 5 and 6, cf. Baradaran et al. 2013). The hydrophilic site would instead correspond to the part of the chamber that accommodates the ubiquinol product, intrinsically more hydrophilic than the oxidized form. Consequently, hydrophilic quinones would preferentially react with this site in competition with endogenous QH_2, whereas hydrophobic quinones would not bind to the same site until fully reduced. Short-chain Q homologs such as Q-2 are likely to bind to both sites simultaneously (Degli Esposti et al. 1996), even if they may have slightly different affinity for one site or the other, as suggested by their enzymatic properties in mutants of Q-binding Y87 (Tocilescu et al. 2010a,b). The chemically similar piericidin A (fig. 6) appears instead to have equivalent binding affinity for both sites in complex I (Gutman et al. 1970; Grivennikova et al. 2003). Of note, the binding data of Okun et al (1999) would be compatible with two piericidin binding sites too, by considering the over-estimation of complex I content in their bovine mitochondrial particles (0.06 nmol per mg of protein, whereas the normal content in the same particles is 0.03–0.04 nmol per mg of protein; Gutman et al. 1970).

The above re-definition of the old concept of two Q reaction sites can be extended to the classification of the large variety of Q antagonists of complex I, previously defined as class I and II (Friedrich et al. 1994) or type A and B (Degli Esposti 1998) inhibitors. Most of such inhibitors can now be re-considered as a single category of chemically different compounds that share the capacity of interacting with both the distal and the hydrophilic Q site. In other words, they effectively have two interaction sites in complex I like Q-2, even if they reach these sites from a common entrance in the complex. Only a few compounds such as rolliniastatins would not compete or overlap with type C inhibitors, a category of compounds introduced by this Author and co-workers (Degli Esposti et al. 1994; Andreani et al. 1995; Degli Esposti 1998) to account for complex I inhibition by myxothiazol and chemicals competing with ubiquinol (Degli Esposti et al. 1993a,b; Degli Esposti et al. 1994).

The above characteristics can now be rationalized in molecular terms by considering the mapping of resistance sites to myxococcal antibiotics and capsaicin, which overlap the

second domain of piericidin resistance and many resistance sites for rotenone and quinazoline inhibitors, but not the first domain of piericidin resistance that roughly corresponds to the distal Q site (fig. 6 and table 3). Type C inhibitors, instead, predominantly interact with the hydrophilic Q site in complex I, a concept that introduces a simplified classification of complex I inhibitors following its evolution for adapting to natural Q substrates. This re-classification of inhibitors would not be inconsistent with the evidence that a single molecule of piericidin A is bound to *Thermus* complex I (Baradaran et al. 2013), because piericidin sensitivity in *Thermus* membranes is approximately one-order of magnitude lower than in mammalian mitochondria (Meinhardt et al. 1990 cf. Degli Esposti 1998). Consequently, the second interaction site of the inhibitor is likely to be weaker in *Thermus* than in mammals or other bacteria (Grivennikova et al. 2003), perhaps owing to unusual substitutions in the NuoD subunit such as A to P at position 391 (fig. 4*B*). The same substitution occurs in the 49-kDa subunit of *Yarrowia* complex I, which has limited sensitivity to piericidin (Kerscher et al. 1999) compared with closely related fungi such as *Cyberlindnera fabiamii* (formerly *Candida utilis*; Coles et al. 1974) having A at position 391 of the same subunit (not shown).

The final conclusion regards the new light that this work is throwing on the evolutionary pattern of complex I following major changes in its function. From the ancestral Nuo complexes retaining the *mbx* function of transferring electrons from reduced ferredoxin to NADP+, Fpo complexes developed the earliest acquisition of Q reactivity with Mph, which then evolved into MQ- or PQ- oxidoreductase enzymes in photosynthetic *Chlorobi* and Cyanobacteria. Oxidation of NADH arrived later, once the N-module was incorporated into the initial NUO11 operon (figs. 1*B* and 2). Overall, complex I has thus changed its function three times before becoming the huge bioenergetic machine we are familiar with. While maintaining the same core structure, local sequence variation in key subunits of the complex has occurred multiple times for adapting to changes in substrates or acquiring inhibitor resistance. These variations have been discerned here to produce insightful structure–function correlations that can now be tested experimentally, either by enlarging the sequence information currently available or undertaking focused functional studies.

Methods

The approaches followed in this work mostly derived from those recently introduced for studying the evolution of mitochondria and bacterial terminal oxidases (Degli Esposti et al. 2014, 2015). In essence, the program Domain Enhanced Lookup time Accelerated BLAST, DELTABLAST (Boratyn et al. 2012), has been used to investigate Nuo proteins in the National Center for Biotechnology Information (NCBI) resources. Alignments of protein sequences have been refined manually from initial drafts obtained with the COBALT resource of the DELTABLAST program (Degli Esposti et al. 2014), complemented with phylogenetic trees obtained with the program PhyML 3.0.

Given the variety in the composition and sequence of *nuo* operons in prokaryotes (Moparthi and Hägerhäll 2011; Marreiros et al. 2013; Spero et al. 2015), the principal types of gene clusters for bacterial complex I have been identified systematically with the simple annotation of the number of their single-copy subunits. The complete set of these subunits is 14 for the majority of alpha, beta, and gamma proteobacteria (Spero et al. 2015) and therefore, their operon is named NUO14. NUO13 is instead the complete operon for the subset of alpha and gamma proteobacteria, including *E. coli*, which have NuoD fused with NuoC, whereas NUO12 corresponds to complete operons exhibiting the additional fusion of NuoD with NuoB, as in some deltaproteobacteria (Marreiros et al. 2013; Spero et al. 2015—cf. supplementary fig. S2, Supplementary Material online). Organisms possessing operons lacking the N module of the NuoE-G subunits within their genome are considered to have the ancestral NUO11 operon (or NUO10 when NuoD is fused to NuoC, as in Nautiliales). Intermediate combinations resulting from additional copies of one subunit are labeled NUO11+, that subunit, for instance, NUO11+M for the operon of *Desulfovibrio africanus* (supplementary fig. S2, Supplementary Material online), whereas combinations that derive from the loss of one or more subunits from a primordial NUO14 cluster are labeled NUO14minus, the missing subunit. When the operon is separated in different sub-clusters, it is defined as split, as, for instance, in the case of *Bdellovibrio* (supplementary fig. S2, Supplementary Material online). Detailed phylogenetic analysis has indicated that, with the exception of Nautiliales, the various gene clusters present in epsilon proteobacteria (Weerakoon and Olson 2008; Marreiros et al. 2013) fall in this category of derived operons (fig. 1 and data not shown) and therefore cannot be considered as possible intermediates in the evolution of the complete Nuo enzyme as previously considered (Moparthi and Haggerwall 2011). The style reported by T. Yagi and co-workers (Sinha et al. 2015) has been used for the protein subunits of bacterial complex I, for example, NuoD. For proteins that are coded also in mtDNA, the bacterial definition has been combined with the nomenclature of the corresponding mitochondrial gene (e.g., Nad7 for NuoD), as well as the original classification of bovine subunits introduced by J. Walker and colleagues (e.g., 49 kDa for NuoD; Fearnley and Walker 1992).

Three-dimensional images of the crystal structure of the entire respiratory complex I of *Thermus* (Baradaran et al. 2013) have been obtained with the program CCP4MG, version 2.10.4. Chemical structures of inhibitors and quinones were obtained with the program JChem (ChemAxon.com). Bioinformatic data have been integrated with available biochemical and microbiological information, including unpublished data on complex I activities, which were obtained in

coupled and NADH-activated submitochondrial particles from bovine heart following the methods described earlier (Degli Esposti et al. 1994; Degli Esposti et al. 1996).

Supplementary Material

Supplementary figures S1–S3 are available at *Genome Biology and Evolution* online (http://www.gbe.oxfordjournals.org/).

Acknowledgments

The author thanks Anna Ghelli (Bologna University) and Anna Ngo (Monash University) for technical assistance in the functional experiments, Diego Gonzalez-Halphen (Universitad National Autonoma de Mexico) for critical reading of the manuscript, and Esperanza Martinez-Romero and Lucero Y. Rivera-Najera (Center for Genomic Sciences, University Autonoma de Mexico, Cuernavaca) for their help and support in revising the paper. Roberto Cingolani is kindly thanked for financial support with intramural IIT funds.

Literature Cited

Abken HJ, et al. 1998. Isolation and characterization of methanophenazine and function of phenazines in membrane-bound electron transport of *Methanosarcina mazei* Gö1. J Bacteriol. 180(8):2027–2032.

Andreani A, Rambaldi M, Leoni A, Locatelli A, Ghelli A et al. 1995. Thienylimidazo[2,1-b]thiazoles as inhibitors of mitochondrial NADH dehydrogenase. J Med Chem. 38:1090–1097.

Aussel L, et al. 2014. Biosynthesis and physiology of coenzyme Q in bacteria. Biochim Biophys Acta. 1837:1004–1011.

Bapteste E, et al. 2008. Alternative methods for concatenation of core genes indicate a lack of resolution in deep nodes of the prokaryotic phylogeny. Mol Biol Evol. 25:83–91.

Baradaran R, Berrisford JM, Minhas GS, Sazanov LA. 2013. Crystal structure of the entire respiratory complex I. Nature 494:443–448.

Battchikova N, Eisenhut M, Aro EM. 2011. Cyanobacterial NDH-1 complexes: novel insights and remaining puzzles. Biochim Biophys Acta. 1807:935–944.

Baumer S, et al. 2000. The F420H2 dehydrogenase from *Methanosarcina mazei* is a redox-driven proton pump closely related to NADH dehydrogenases. J Biol Chem. 275:17968–17973.

Berry EA, Zhang Z, Huang LS, Kim SH. 1999. Structures of quinone-binding sites in bc complexes: functional implications. Biochem Soc Trans. 27:565–72.

Boratyn GM, et al. 2012. Domain enhanced lookup time accelerated BLAST. Biol Direct. 7:12.

Borodina I, Krabben P, Nielsen J. 2005. Genome-scale analysis of *Streptomyces coelicolor* A3(2) metabolism. Genome Res. 15:820–829.

Brandt U. 2006. Energy converting NADH:quinone oxidoreductase (complex I). Annu Rev Biochem. 75:69–92.

Bridger SL, et al. 2011. Deletion strains reveal metabolic roles for key elemental sulfur-responsive proteins in Pyrococcus furiosus. J Bacteriol. 193:6498–6504.

Brierley E, Smith HJ. 1968. A high content (minus)-deguelin concentrate from a commercial derris resin by steady-state distribution. J Pharm Pharmacol. 20:840–844.

Burger G, Gray MW, Forget L, Lang BF. 2013. Strikingly bacteria-like and gene-rich mitochondrial genomes throughout jakobid protists. Genome Biol Evol. 5:418–438.

Campbell BJ, Cary SC. 2004. Abundance of reverse tricarboxylic acid cycle genes in free-living microorganisms at deep-sea hydrothermal vents. Appl Environ Microbiol. 70:6282–6289.

Campbell BJ, et al. 2009. Adaptations to submarine hydrothermal environments exemplified by the genome of Nautilia profundicola. PLoS Genet. 5:e1000362.

Chen Y, et al. 2014. Elucidating hydroxylation and methylation steps tailoring piericidin A1 biosynthesis. Org Lett. 16:736–739.

Coles CJ, Gutman M, Singer TP. 1974. On the reaction of piericidin A with the reduced nicotinamide adenine dinucleotide dehydrogenase of *Candida utilis*. J Biol Chem. 249:3814–3818.

Coppi MV. 2005. The hydrogenases of *Geobacter sulfurreducens*: a comparative genomic perspective. Microbiology 151(Pt 4): 1239–54.

Darrouzet E, Issartel JP, Lunardi J, Dupuis A. 1998. The 49-kDa subunit of NADH-ubiquinone oxidoreductase (Complex I) is involved in the binding of piericidin and rotenone, two quinone-related inhibitors. FEBS Lett. 431:34–38.

Degli Esposti M. 1998. Inhibitors of NADH-ubiquinone reductase: an overview. Biochim Biophys Acta. 1364:222–235.

Degli Esposti M, et al. 1993a. Mitochondrial cytochrome b: evolution and structure of the protein. Biochim Biophys Acta. 1143:243–271.

Degli Esposti M, et al. 1993b. Complex I and complex III of mitochondria have common inhibitors acting as ubiquinone antagonists. Biochim Biophys Res Commun. 190:1090–1096.

Degli Esposti M, et al. 1996. The specificity of mitochondrial complex I for ubiquinones. Biochem J. 313:327–334.

Degli Esposti M, et al. 2014. Evolution of mitochondria reconstructed from the energy metabolism of living bacteria. PLoS One 9:e96566.

Degli Esposti M, et al. 2015. Molecular evolution of cytochrome bd oxidases across proteobacterial genomes. Genome Biol Evol. 7:801–820.

Degli Esposti M, Ghelli A. 1999. Ubiquinone and inhibitor sites in complex I: one, two or three? Biochem Soc Trans 27:60660–9.

Degli Esposti M, Ghelli A, Ratta M, Cortes D, Estornell E. 1994. Natural substances (acetogenins) from the family Annonaceae are powerful inhibitors of mitochondrial NADH dehydrogenase (Complex I). Biochem J. 301:161–167.

Drennan CL, Heo J, Sintchak MD, Schreiter E, Ludden PW. 2001. Life on carbon monoxide: X-ray structure of *Rhodospirillum rubrum* Ni-Fe-S carbon monoxide dehydrogenase. Proc Natl Acad Sci U S A. 98:11973–11978.

Dupuis A, et al. 1998. The complex I from *Rhodobacter capsulatus*. Biochim Biophys Acta. 1364:147–165.

Efremov RG, Sazanov LA. 2012. The coupling mechanism of respiratory complex I - a structural and evolutionary perspective. Biochim Biophys Acta. 1817:1785–1795.

Fato R, et al. 1996. Steady-state kinetics of the reduction of coenzyme Q analogs by complex I (NADH:ubiquinone oxidoreductase) beef heart mitochondria and submitochondrial particles. Biochemistry. 35:2705–2716.

Fearnley IMWalker JE. 1992. Conservation of sequences of subunits of mitochondrial complex I and their relationships with other proteins. Biochim Biophys.Acta. 1140:105–134.

Fendel U, Tocilescu MA, Kerscher S, Brandt U. 2008. Exploring the inhibitor binding pocket of respiratory complex I. Biochim Biophys Acta. 1777:660–665.

Friedrich T, Scheide D. 2000. The respiratory complex I of bacteria, archaea and eukarya and its module common with membrane-bound multisubunit hydrogenases. FEBS Lett. 479:1–5.

Friedrich T, et al. 1994. Two binding sites of inhibitors in NADH: ubiquinone oxidoreductase (complex I). Relationship of one site with the ubiquinone-binding site of bacterial glucose:ubiquinone oxidoreductase. Eur J Biochem. 219:691–698.

Galkin A, et al. 2008. Identification of the mitochondrial ND3 subunit as a structural component involved in the active/deactive enzyme transition of respiratory complex I. J Biol Chem. 283:20907–20913.
Gao X, et al. 2003. Structural basis for the quinone reduction in the bc1 complex: a comparative analysis of crystal structures of mitochondrial cytochrome bc1 with bound substrate and inhibitors at the Qi site. Biochemistry. 42:9067–9080.
Ghelli A, et al. 1992. Cytochrome b of protozoan mitochondria: relationships between function and structure. Comp Biochem Physiol B. 103:329–338.
Giovannelli D, et al. 2012. Complete genome sequence of *Thermovibrio ammonificans* HB-1(T), a thermophilic, chemolithoautotrophic bacterium isolated from a deep-sea hydrothermal vent. Stand Genomic Sci. 7:82–90.
Göker M, et al. 2011. Complete genome sequence of the thermophilic sulfur-reducer *Desulfurobacterium thermolithotrophum* type strain (BSA(T)) from a deep-sea hydrothermal vent. Stand Genomic Sci. 5:407–415.
Grivennikova VG, Roth R, Zakharova NV, Hägerhäll C, Vinogradov AD. 2003. The mitochondrial and prokaryotic proton-translocating NADH:ubiquinone oxidoreductases: similarities and dissimilarities of the quinone-junction sites. Biochim Biophys Acta. 1607:79–90.
Gutman M, Singer TP, Casida JE. 1970. Studies on the respiratory chain-linked reduced nicotinamide adenine dinucleotide dehydrogenase. XVII. Reaction sites of piericidin A and rotenone. J Biol Chem. 245:1992–1997.
Hedderich, R. 2004. Energy-converting [NiFe] hydrogenases from archaea and extremophiles: ancestors of complex I. J. Bioenerg. Biomembr. 36:65–75.
Helfenbaum L, et al. 1997. Proton pumping of mitochondrial complex I: differential activation by analogs of ubiquinone. J Bioenerg Biomembr. 29:1–80.
Heo J, Wolfe MT, Staples CR, Ludden PW. 2002. Converting the NiFeS carbon monoxide dehydrogenase to a hydrogenase and a hydroxylamine reductase. J Bacteriol. 184:5894–5897.
Herter SM, Kortlüke CM, Drews G. 1998. Complex I of *Rhodobacter capsulatus* and its role in reverted electron transport. Arch Microbiol. 169:98–105.
Hiraishi A Hoshino Y. 1984. Distribution of rhodoquinone in Rhodospirillaceae and its taxonomic implications. J Gen Appl Microbiol. 30:435–448.
Hollingworth RM, Ahammadsahib KI, Gadelhak G, McLaughlin JL. 1994. New inhibitors of complex I of the mitochondrial electron transport chain with activity as pesticides. Biochem Soc Trans. 22:230–233.
Hu P, Lv J, Fu P, Hualing M. 2013. Enzymatic characterization of an active NDH complex from *Thermosynechococcus elongatus*. FEBS Lett. 587:2340–2345.
Huntley S, et al. 2011. Comparative genomic analysis of fruiting body formation in Myxococcales. Mol Biol Evol. 28:1083–1097.
Iizuka T, et al. 2003. *Plesiocystis pacifica* gen. nov., sp. nov., a marine myxobacterium that contains dehydrogenated menaquinone, isolated from the Pacific coasts of Japan. Int J Syst Evol Microbiol. 53:189–195.
Iommarini L, Calvaruso MA, Kurelac I, Gasparre G, Porcelli AM. 2013. Complex I impairment in mitochondrial diseases and cancer: parallel roads leading to different outcomes. Int J Biochem Cell Biol. 45:47–63.
Kashani-Poor N, Zwicker K, Kerscher S, Brandt U. 2001. A central functional role for the 49-kDa subunit within the catalytic core of mitochondrial complex I. J Biol Chem. 276:24082–24087.
Kazakoff SH, et al. 2012. Capturing the biofuel wellhead and powerhouse: the chloroplast and mitochondrial genomes of the leguminous feedstock tree *Pongamia pinnata*. PLoS One 7:e51687.
Kerscher SJ, Okun JG, Brandt U. 1999. A single external enzyme confers alternative NADH:ubiquinone oxidoreductase activity in *Yarrowia lipolytica*. J Cell Sci. 112:2347–2354.
Kraiczy P, et al. 1996. The molecular basis for the natural resistance of the cytochrome bc1 complex from strobilurin-producing basidiomycetes to center Qp inhibitors. Eur J Biochem. 235:54–63.
Kunze B, et al. 1992. Phenoxan, a new oxazole-pyrone from myxobacteria: production, antimicrobial activity and its inhibition of the electron transport in complex I of the respiratory chain. J Antibiot. (Tokyo) 45:1549–1552.
Lang K, et al. 2015. New mode of energy metabolism in the seventh order of methanogens as revealed by comparative genome analysis of "*Candidatus methanoplasma termitum*". Appl Environ Microbiol. 81:1338–1352.
Lenaz G, Daves GD, Folkers K. 1968. Organic structural specificity and sites of coenzyme Q in succinoxidase and DPNH-oxidase systems. Arch Biochem Biophys. 123:539–550.
Löw H, Alm B, Vallin I. 1964. The use of phenazine methosulfate in the study of oxidative phosphorylation. Biochem Biophys Res Commun. 14:347–352.
Lücker S, Nowka B, Rattei T, Spieck E, Daims H. 2013. The genome of *Nitrospina gracilis* illuminates the metabolism and evolution of the major marine nitrite oxidizer. Front Microbiol. 4:27.
Ma W, Ogawa T. 2015. Oxygenic photosynthesis-specific subunits of cyanobacterialNADPH dehydrogenases. IUBMB Life. 67:3–8.
Magnitsky S, et al. 2002. EPR characterization of ubisemiquinones and iron-sulfur cluster N2, central components of the energy coupling in the NADH-ubiquinone oxidoreductase (complex /I) in situ. J Bioenerg Biomembr. 34:193–208.
Marreiros BC, Batista AP, Duarte AM, Pereira MM. 2013. A missing link between complex I and group 4 membrane-bound [NiFe] hydrogenases. Biochim Biophys Acta. 1827:198–209.
Masuya T, Murai M, Ifuku K, Morisaka H, Miyoshi H. 2014. Site-specific chemical labeling of mitochondrial respiratory complex I through ligand-directed tosylate chemistry. Biochemistry 53:2307–2317.
Meinhardt SW, et al. 1990. Studies on the NADH-menaquinone oxidoreductase segment of the respiratory chain in *Thermus thermophilus* HB-8. J Biol Chem. 265:1360–1368.
Mills SD, Yang W, MacCormack K. 2004. Molecular characterization of benzimidazole resistance in *Helicobacter pylori*. Antimicrob Agents Chemother. 48:2524–2530.
Moparthi VK, Hagerhall C. 2011. The evolution of respiratory chain complex I from a smaller last common ancestor consisting of 11 protein subunits. J Mol Evol. 72:484–497.
Morgan JB, et al. 2010. The marine sponge metabolite mycothiazole: a novel prototype mitochondrial complex I inhibitor. Bioorg Med Chem. 18:5988–5994.
Müller M, et al. (2012) Biochemistry and evolution of anaerobic energy metabolism in eukaryotes. Microbiol Mol Biol Rev. 76:444–495.
Murai M, Sekiguchi K, Nishioka T, Miyoshi H. 2009. Characterization of the inhibitor binding site in mitochondrial NADH-ubiquinone oxidoreductase by photoaffinity labeling using a quinazoline-type inhibitor. Biochemistry 48:688–698.
Nelson ME, et al. 2005. Cytochrome b6 arginine 214 of *Synechococcus sp.* PCC 7002, a key residue for quinone-reductase site function and turnover of the cytochrome bf complex. J Biol Chem. 280:10395–10402.
Nelson-Sathi S, et al. 2015. Origins of major archaeal clades correspond to gene acquisitions from bacteria. Nature. 517:77–80.
Ngandeu F, et al. 2008. Rotenoid derivatives and other constituents of the twigs of *Millettia duchesnei*. Phytochemistry 69:258–263.
Oda Y, et al. 2008. Multiple genome sequences reveal adaptations of a phototrophic bacterium to sediment microenvironments. Proc Natl Acad Sci U S A. 2008 105:18543–18548.
Oh JI, Bowien B. 1998. Structural analysis of the fds operon encoding the NAD+-linked formate dehydrogenase of *Ralstonia eutropha*. J Biol Chem. 273:26349–26360.

Ohshima M, et al. 1998. Characterization of the ubiquinone reduction site of mitochondrial complex I using bulky synthetic ubiquinones. Biochemistry 37:6436–6445.
Okun JG, Lümmen P, Brandt U. 1999. Three classes of inhibitors share a common binding domain in mitochondrial complex I (NADH:ubiquinone oxidoreductase). J Biol Chem. 274:2625–2630.
Ouchane S, Agalidis I, Astier C. 2002. Natural resistance to inhibitors of the ubiquinol cytochrome c oxidoreductase of *Rubrivivax gelatinosus*: sequence and functional analysis of the cytochrome bc(1) complex. J Bacteriol. 184:3815–3822.
Pohl T, et al. 2007. Iron-sulfur cluster N7 of the NADH:ubiquinone oxidoreductase (complex I) is essential for stability but not involved in electron transfer. Biochemistry 46:6588–6596.
Putnam NH, et al. 2007. Sea anemone genome reveals ancestral eumetazoan gene repertoire and genomic organization. Science 317:86–94.
Reichenbach H, Gerth K, Irschik H, Kunze B, Hofle G. 1988. Myxobacteria: a source of new antibiotics. Trends Biotechnol. 6:115–121.
Ruzicka FJ, Crane FL. 1970. Quinone interaction with the respiratory chain-linked NADH dehydrogenase of beef heart mitochondria. Biochim Biophys Acta. 223:71–85.
Sazanov LA. 2015. A giant molecular proton pump: structure and mechanism of respiratory complex I. Nat Rev Mol Cell Biol. 16:375–388.
Sazanov LA, Hinchliffe P. 2006. Structure of the hydrophilic domain of respiratory complex I from *Thermus thermophilus*. Science 311: 1430–1436.
Schübbe S, et al. 2009. Complete genome sequence of the chemolithoautotrophic marine magnetotactic coccus strain MC-1. Appl Environ Microbiol. 75:4835–4852.
Schuler F, et al. 1999. NADH-quinone oxidoreductase: PSST subunit couples electron transfer from iron-sulfur cluster N2 to quinone. Proc Natl Acad Sci U S A. 96:4149–4153.
Schütz M, et al. 2003. The naphthoquinol oxidizing cytochrome bc1 complex of the hyperthermophilic knallgasbacterium *Aquifex aeolicus*: properties and phylogenetic relationships. Biochemistry 42: 10800–10808.
Segata N, Börnigen D, Morgan XC, Huttenhower C. 2013. PhyloPhlAn is a new method for improved phylogenetic and axonomic placement of microbes. Nat Commun. 4:2304.
Sharma P, Teixeira de Mattos MJ, Hellingwerf KJ, Bekker M. 2012. On the function of the various quinone species in *Escherichia coli*. FEBS J. 279:3364–3373.
Sharma V, et al. 2015. Redox-induced activation of the proton pump in the respiratory complex I. Proc Natl Acad Sci U S A. 112:11571–11576.
Shimada H, Shida Y, Nemoto N, Oshima T, Yamagishi A. 2001. Quinone profiles of *Thermoplasma acidophilum* HO-62. J Bacteriol. 183: 1462–1465.
Shimomura Y, Kawada T, Suzuki M. 1989. Capsaicin and its analogs inhibit the activity of NADH-coenzyme Q oxidoreductase of the mitochondrial respiratory chain. Arch Biochem Biophys. 270:573–577.
Simin K, Ali Z, Khaliq-Uz-Zaman SM, Ahmad VU. 2002. Structure and biological activity of a new rotenoid from *Pongamia pinnata*. Nat Prod Lett. 16:351–357.
Singer TP, Ramsay RR. 1994. The reaction sites of rotenone and ubiquinone with mitochondrial NADH dehydrogenase. Biochim Biophys Acta. 1187:198–202.
Sinha PK, et al. 2015. Conserved amino acid residues of the NuoD segment important for structure and function of *Escherichia coli* NDH-1 (complex I). Biochemistry 54:753–764.
Spero MA, Aylward FO, Currie CR, Donohue TJ. 2015. Phylogenomic analysis and predicted physiological role of the proton-translocating NADH:quinone oxidoreductase (complex I) across bacteria. mBio 6:e00389–15.
Sprecher BN, Gittings ME, Ludwig RA. 2012. Respiratory membrane endohydrogenase activity in the microaerophile *Azorhizobium caulinodans* is bidirectional. PLoS One 7:e36744.
Srivastava M, et al. 2010. The *Amphimedon queenslandica* genome and the evolution of animal complexity. Nature 466:720–726.
Surup F, Shojaei H, von Zezschwitz P, Kunze B, Grond S. 2008. Iromycins from *Streptomyces sp.* and from synthesis: new inhibitors of the mitochondrial electron transport chain. Bioorg Med Chem. 16: 1738–1746.
Suzuki A, Knaff DB. 2005. Glutamate synthase: structural, mechanistic and regulatory properties, and role in the amino acid metabolism. Photosynth Res. 83:191–217.
Sztukowska M, Bugno M, Potempa J, Travis J, Kurtz DM Jr. 2002. Role of rubrerythrin in the oxidative stress response of *Porphyromonas gingivalis*. Mol Microbiol. 44:479–488.
Takahashi N, Suzuki A, Tamura S. 1965. Structure of piercidin a. J Am Chem Soc. 87:2066–2068.
Tocilescu MA, Fendel U, Zwicker K, Kerscher S, Brandt U. 2007. Exploring the ubiquinone binding cavity of respiratory complex I. J Biol Chem. 282:29514–29520.
Tocilescu MA, et al. 2010a. The role of a conserved tyrosine in the 49-kDa subunit of complex I for ubiquinone binding and reduction. Biochim Biophys Acta. 1797:625–632.
Tocilescu MA, Zickermann V, Zwicker K, Brandt U. 2010b. Quinone binding and reduction by respiratory complex I. Biochim Biophys Acta. 1797:1883–1890.
Turner JM, Messenger AJ. 1986. Occurrence, biochemistry and physiology of phenazine pigment production. Adv Microb Physiol. 27:211–275.
Van Hellemond JJ, Klockiewicz M, Gaasenbeek CP, Roos MH, Tielens AG. 1995. Rhodoquinone and complex II of the electron transport chain in anaerobically functioning eukaryotes. J Biol Chem. 270: 31065–31070.
Verkhovsky M, Bloch DA, Verkhovskaya M. 2012. Tightly-bound ubiquinone in the *Escherichia coli* respiratory complex I. Biochim Biophys Acta. 1817:1550–1556.
Vignais PM, Billoud B. 2007. Occurrence, classification, and biological function of hydrogenases: an overview. Chem Rev. 107:4206–4272.
Vinothkumar KR, Zhu J, Hirst J. 2014. Architecture of mammalian respiratory complex I. Nature 515:80–84.
Weerakoon DR, Olson JW. 2008. The *Campylobacter jejuni* NADH:ubiquinone oxidoreductase (complex I) utilizes flavodoxin rather than NADH. J Bacteriol. 190:915–925.
Welte C, Deppenmeier U. 2014. Bioenergetics and anaerobic respiratory chains of aceticlastic methanogens. Biochim Biophys Acta. 1837:1130–1147.
Yagi T, Yano T, Di Bernardo S, Matsuno-Yagi A. 1998. Procaryotic complex I (NDH-1), an overview. Biochim Biophys Acta. 1364:125–133.
Yamashita T, et al. 2004. Rhodoquinone reaction site of mitochondrial complex I, in parasitic helminth, *Ascaris suum*. Biochim Biophys Acta. 1608:97–103.
Yip CY, Harbour ME, Jayawardena K, Fearnley IM, Sazanov LA. 2011. Evolution of respiratory complex I: "supernumerary" subunits are present in the alpha-proteobacterial enzyme. J Biol Chem. 286:5023–5033
Zickermann V, et al. 2015. Structural biology. Mechanistic insight from the crystal structure of mitochondrial complex I. Science 347:44–49.

Associate editor: Bill Martin